Metabolic Divergence of Aged Tenocytes:

Insights into Tendinopathic Disease Progression

A Thesis

Presented to

the faculty of the School of Engineering and Applied Science

University of Virginia

---

in partial fulfillment

of the requirements for the degree

Master of Science

by

William Patterson

May 2013

APPROVAL SHEET

The thesis

is submitted in partial fulfillment of the requirements

for the degree of

Master of Science

AUTHOR

The thesis has been read and approved by the examining committee:

Joseph Park

Advisor

Shayn Peirce-Cottler

Zhen Yan

Gary Balian

Accepted for the School of Engineering and Applied Science:

Dean, School of Engineering and Applied Science

May

2013

Acknowledgements:

This project was only possible due to the support and hard work of many people, who have played a pivotal role in my research project over the last 2 years. I am sincerely grateful and it was truly an honor to work with you.

First, I must thank Dr. Joseph Park, my advisor and the principal investigator of this project. Dr. Park was confident in my abilities as a researcher and student since the first day I stepped into his office. He provided me with an opportunity that made my graduate experience possible. He then continued to provide guidance, vision, and encouragement to drive this project forward.

To my thesis committee consisting of Dr. Shayn Peirce-Cottler, Dr. Gary Balian, and Dr. Zhen Yan, I am grateful for your guidance and critique that was essential to questioning my hypothesis, developing new insights, and strengthening my research as a whole.

To Dr. Ching-Hua Yeh, I could not ask for a more committed mentor. I am thankful for your guidance in the lab. I simply would not have been able to accomplish this work without your help.

To Dr. Shaharyar Khan, Dr. Francisco Portel, Dr. Jameel Dennis, and Dr. Isaac Onyango, thank you for your time and energy teaching me in the lab. Our collaboration was a key inroad to establishing my project.

To Dr. Kyle Hoehn and Brandon Kenwood, your experimental help was critical to completing my examination of cellular metabolism.

To Dr. Abhijit Dighe, your research knowledge, experimental reasoning, and forthright criticism are truly unmatched in my eyes. You have greatly contributed to my work through your critique and enthusiasm, thank you.

To Dr. Jan Redick and Dr. Stacy Guillot, your contributions and knowledge of advanced microscopy techniques was a great help to several aspects of my project.

To Sheri VanHoose, I am grateful for your assistance in preparing my tissue histology work.

To Gina Beck, thank you for helping me to get started in the lab. I appreciate your time and patience in the earliest days of my tenure with the orthopedics lab.

To my lab members in the Department of Orthopedics, thank you for your advice, criticism, guidance, and patience that you kindly exhibited each and every day.

To the Departments of Biomedical Engineering and Orthopedics, the academic community here at UVa is outstanding. The faculty, staff, and students have played an invaluable role in promoting my research experience at UVa.

To my friends and family, I can never thank you enough for providing inspiration and support.

Table of Contents:

Abstract:

Chronic tendinopathies commonly affect physically active patients and can be both painful and debilitating. Clinical observations and research in the field suggest that the etiology of this disease encompasses a complex combination of overuse, injury, and aging. Chronic tendinopathy is characterized by a lack of tissue maintenance resulting in dysfunctional tissue composition with poor architectural organization. The degenerative tissue has altered mechanical properties and consequently, a propensity for a higher incidence of injury.

The native tendon cell population serves as the primary regulator of structural (extracellular matrix) synthesis, remodeling, and repair. These cells are the primary therapeutic targets for non-operative means of alleviating tendinopathic pathology. We aimed to elucidate the role of tendon cell aging on chronic tendinopathy by studying cells that were isolated from tissues of older animals.

In this investigation, progression of tendinopathy was identified in Achilles tendon from aged, 22-month old, rats. Primary tendon cell cultures from the older rats were characterized and these culture systems were utilized in two subsequent studies detailing age-dependent dysfunction. In the first study, the aged cells were examined for fundamental changes in glycolytic and oxidative function to examine the possibility of an age-dependent basis correlating energy metabolism and the lack of tissue maintenance. Although there is no definitive evidence for the role of mitochondrial dysfunction, cells from the older rats display a distinct glycolytic phenotype in comparison to the juvenile tendon cells. In the second study, cell-mediated regulation of tendon architecture was investigated more directly by

examining the age-dependent activity of degradative enzymes responsible for architectural remodeling. We report age-dependent changes in matrix metalloproteinase activities that are consistent with age-related tendon pathology.

List of Figures:

List of Tables:

List of Abbreviations:

APMA: 4-aminophenyl mercuric acetate
ATP: Adenosine triphosphate
CMXRos: Cholormethyl-X-rosamine
COXIV: Cytochrome C Oxidase Subunit IV
C_T: Cycle threshold value
DCFDA: Dichlorodihydrofluorescein diacetate
DIG: Digoxigenin
DMEM: Dulbecco's Modified Eagle Medium
EDTA: Ethylenediaminetetraacetic acid
FBS: Fetal bovine serum
FCCP: Carbonyl cyanide 4-(trifluoromethoxy)phenylhydrazone
F344: Fischer 344
GAG: Glycosminoglycan
JC-1: 5,5',6,6'-Tetrachloro-1,1',3,3'-tetraethyl-imidacarbocyanine iodide
LDH: Lactate dehydrogenase
MMP: Matrix metalloproteinase
NAD+: Nicotinamide adenine dinucleotidePAGE: Polyacrylamide gel electrophoresis
PBS: Phosphate Buffered SalinePLA: Polylactic acid
OCR: Oxygen Consumption Rate
RFU: Relative Fluorescence Units
RNS: Reactive nitrogen species
ROS: Reactive oxygen species
RT-PCR: Reverse transcription polymerase chain reaction
SSC: Saline sodium citrate buffer
TAE: Tris-acetate-EDTA buffer
TEM: Transmission electron microscopy
TGF-β: Transforming Growth Factor Beta
Tris: Tris(hydroxymethyl)aminomethane
UV: Ultraviolet

Part 1: Gross Cell Morphology and Characterization of Primary Rat Achilles Tendon Cells

Introduction:

Tendon is a musculoskeletal tissue responsible for transmitting load between muscle and bone. Type-I collagen accounts for approximately 70% of the dry mass of tendon and is the primary structural component of the tissue[1]. Collagen has a complex hierarchical structure. Starting with the most elementary unit, three collagen polypeptides form a triple helix that is stabilized by hydrogen bonding between the polypeptide chains. The triple helices then associate in a parallel formation to form collagen fibrils. Hydroxyproline and hydroxylysine play critical structural roles in hydrogen bonding between collagen polypeptide chains and crosslinking between triple helices, respectively[2]. Collagen fibrils are typically between 50 and 600 nm in diameter. In tendon development fibril diameters increase, and with advanced aging can reach irregularly large sizes of up to 600 nm[3]. Collagen synthesis is a cell-mediated process that involves terminal polypeptide cleavages and hydroxylation events regulated by tendon fibroblast-like cells [2],[4].

Tendon also has a small, but significant presence of glycoproteins and proteoglycans known as ground substance, which due to significant charge density, maintains the hydrophilicity of the tissue and plays an important role modulating nutrient solubility [2]. The small leucine-rich proteoglycans, including decorin, biglycan, and lumican , have been shown to bind to fibrillar collagen and modulate collagen organization[5]. Specifically, decorin is the most abundant tendon proteoglycan and plays a major role in inhibiting fibrillogenesis [5], [6]. Additionally, decorin has been shown to sequester transforming growth factor beta (TGF-β) and

regulate cellular proliferation [7]. The proteoglycan content of tendon plays a significant role in remodeling and repair via the regulation of both matrix maturation and cellular signaling.

Tenocytes makeup about 90% of the cells in mature tendon and participate in repair and maintenance of the tissue. These cells are fibroblast-like with elongated cell bodies and numerous spindle-shaped extensions [8]. Tenocytes are arranged as longitudinal sheets and extend around collagen fibrils forming a complex network of finger-like processes. The unique arrangement of tenocytes within the tendon allows these cells to come in close contact with the collagen fibrils, which is essential to proper tissue remodeling. Tenocytes are primarily responsible for the synthesis, deposition, alignment, and turnover of collagen fibrils in mature tendon. They also synthesize all other extracellular components native to the tendon tissue including other, nonfibrillar collagens, proteoglycans, and glycosaminoglycans (GAGs) [9]. Tenocytes are responsive to both stress and injury and are metabolically activated once they have migrated to the repair site. Tenocytes normally maintain a fine balance between matrix production and degradation; during wound healing this balance is systematically shifted in both directions to allow for synthesis and then tissue remodeling [10].

Several characteristic changes occur in cellular and matrix function during aging. Additionally, aging has been identified as an intrinsic risk factor of tendinopathy[11]. These age-dependent changes have been detected as early as the third decade of life[12]. The cellular density of the tendon has been shown to decrease, the cells become longer and more slender, and the nucleus to cytoplasm ratio increases[12]. The proliferative ability of aged tenocytes in culture has been reported to decrease in association with the progression of senescence[13]. Moreover, matrix composition changes drastically. The proteoglycan and associated water

content are diminished, thus increasing the relative amount of collagen, which is more or less unchanged[12]. Collagen fibrils become irreversibly cross-linked, resulting in tissue that is resistant to degradation. Collagen disorganization and mechanical degradation lead to more rigid collagen fibrils with decreased tensile strength[12]. Degenerative changes in both the native cell population and constitutive matrix result in a weaker tissue that is more prone to injury and has inferior healing potential.

The aim of the first part of this investigation was two-fold. First, we characterized the proliferation and morphology of the isolated tendon cells in vitro. This characterization served to establish the baseline growth rates for other experiments that were examined in part 2 of this study. The characterization also verified the potential therapeutiuc eligibility of this cell population by addressing replicative senescence as a source of diminished cellular function. Second, age-related, tendinopathic changes were identified in the tissue. Collagen fibril size, tissue organization, and cellular density of the tissue were examined to address the status of tendinopathy in the older rats. Validating the degenerative condition of the tissue offers perspective on the utility of the investigation and provides a basis for determining the clinical relevance of the study. Moreover, in the process of describing the metabolic divergence of aged tendon, this study characterized a clinically valid model to study tendinopathy. The aged rat model was deliberately investigated with the intention of providing a basis for accelerating the process of therapeutic development and elucidating the mechanistic relationships in the pathogenesis of the disease.

Methods:

Cell Culture:

Primary tendon cells were isolated from 22-month and 1-month old Fischer 344 rats to produce populations of aged and juvenile tenocytes, respectively. The 22-month rats represent 92% of the mean F344 lifespan while the 1-month rats represent 4% of the mean F344 lifespan. These age groups were chosen to characterize both ends of the aging spectrum of mature tendon. Fischer rats were used primarily because of availability for the desired age groups and their widespread use in gerontological studies. The age and weight of each rat was recorded at the time of CO_2 asphyxiation. Sterile surgical procedures were followed during the excision of the tendons. The Achilles tendons of both hind limbs were removed and rinsed three times with normal culture media (DMEM-High Glucose, 10% FBS, 1% sodium ascorbate, 1% penicillin/streptomycin, 1 mM sodium pyruvate). The tendons were then cut into approximately 3 mm x 2 mm specimens and scored into tissue culture plastic (12-well plates with 1-2 tissue specimens per well) with a scalpel blade and submerged in growth media. The explant cultures were left to expand for 1 to 2 weeks at 5% CO_2 and 37°C. Culture media with and without glucose were used to determine the effect of glucose starvation. The media without glucose was supplemented with 5mM sodium pyruvate as a substrate for energy metabolism. Cell culture media was replaced every 48-72 hours after the first week of explant growth during which the cells were not disturbed. The explant yields were quantified by combining the cells from each age group (12-wells per age group) and taking three cell count measurements per cell suspension. The cell count methods are detailed below.

Cell Proliferation

Isolated cells were plated in 12-well tissue culture plates at approximately 3000 cells per cm^2 . Cells were rinsed with PBS and lifted with 0.05% Trypsin-EDTA in PBS at 24 hour intervals up to 72 hours. Cell counts were obtained at each interval using a Millipore Scepter 2.0 Automated Cell Counter. The cell counts were done in quadruplicate and the average count was recorded. The data presented below shows the differences in cell number at 72 hours.

Cell Diameter:
The average cell diameter of the cells was also obtained using the Scepter 2.0 and was recorded in conjunction with the proliferation data.

Cell Shape:
Aged and juvenile tenocytes were imaged by inverted light microscopy using the 20x objective of an Axiovert 40 microscope (Carl Zeiss) at 24, 48, and 72 hours after plating. Images were taken with the AxioCam ERc 5s camera at three random locations around each well in order to obtain an unbiased collection of images. Cell parameters of adherent cells were analyzed in ImageJ. Three images from each age group were analyzed and a random sampling of 10 cells from each image was selected for analysis. The spindle axis length, or long axis of the spindle-shaped cells, was measured as well as the perpendicular width of the cells. The nucleus of each cell was identified and measured by approximating each nucleus with an ellipse and recording the perimeter.

Telomere Length:
DNA was isolated from $1x10^6$ cells after pelleting the culture and washing with PBS. Cell lysis, protein digestion, RNA digestion, protein precipitation, and DNA precipitation were carried out in accordance with the manufacturer's instructions (Roche Applied Sciences-DNA Isolation Kit). A DNA sample was then diluted 50X and measured by spectrophotometry. The concentration

and 260/280 value were recorded. The TeloTAGGG Telomere Length Assay (Roche Applied Sciences) was then used to determine the mean telomere restriction fragment length. Briefly, 1-2 µg genomic DNA for each sample was digested. The digested DNA was loaded into a 0.8% agarose gel in TAE Buffer. Gel electrophoresis was run for 3-4 hours in TAE running buffer. The migration of DNA was checked by including .01% ethidium bromide in the gel and then visualizing under UV light. The DNA samples in the gel were washed, denatured and transferred over night to a nylon membrane by Southern transfer in 20X SSC. After the transferred DNA was fixed by UV-crosslinking (120mJ), the membrane was hybridized for 3 hours with the telomere probe provided by the kit, incubated with Anti-DIG probe, and detected by X-Ray film exposure. One to five minutes of luminescence exposure was sufficient for accurate quantification. The developed x-ray film was then scanned using a film scanner (Canon), and the images were assessed using ImageJ to subtract background and quantify signal intensity. Quantification was done according to the recommendation from this kit for assessing mean telomere restriction fragment length (TRF).

Collagen Fibril Perimeter:

Hind-limb Achilles tendons were excised from 1-month and 22-month old Fischer 344 rats. The tendons were cut to include 1 mm of the proximal muscle-aponeurosis junction, in other words the tendon was transected proximally 1 mm above the muscle-tendon junction to include approximately 1 mm of muscle-aponeurosis junction. At the distal end, the tendon was transected approximately 1mm above the calcaneal insertion. Muscle was then cleaned from the tendon by dissection. The excised tendons were cut in half, transverse cross-section, at the tendon midsubstance. The tissue was fixed in 2.5% Glutaraldehyde/ 4% Paraformaldehyde. The tendons were then sectioned starting from the midsubstance toward the muscle tendon

junction (to ensure sections were being taken from the midsubtance of the tendon) and imaged by Transmission Electron Microscopy by personnel in the Advanced Microscopy Center. Images of the tendon fibrils at 20,000X magnification were used for quantification of the fibril perimeter distributions. One-hundred random fibril measurements from 4 separate images of 2 individual tendons were made to produce a distribution of fibril perimeters. Fibrils were more accurately approximated by ellipses rather than circles and were measured as perimeter values as opposed to diameter measurements. The distribution of fibril perimeters is shown in the results section below.

Tissue Cellularity:

Tendons were excised as described previously. The tissue was fixed in 4% paraformaldehyde for over 48 hours. Specimens were embedded in paraffin and sectioned with a microtome; both cross-sections and longitudinal sections were prepared. The sections were stained with Hematoxylin/Eosin and imaged using a 40x objective on a reflected light microscope. The embedding, sectioning, and staining was performed by the Tissue Histology Core Lab at the University of Virginia. Cellular density within the tissue was determined by evaluating three separate sections of 2 different tendon samples at 40x magnification for each age group. The nuclei were counted in a 0.0906 mm^2 area at a random location using the cell counting module in ImageJ and the data plotted using the average of three counts for each age group. Longitudinal sections were used to count the nuclei because the cross sections were much smaller and subject to mechanical spreading by the microtome blade, leading to high variability between sections.

Statistical Analysis:

Single statistical comparisons between the 22-month and 1-month groups were assessed by two-tailed T-test, assuming unequal variances between samples. Multiple comparisons, between groups with regard to media condition and animal age, were analyzed by two-tailed two-way ANOVA using IBM SPSS Statistics 20. Before applying the analysis of variance, the sample groups were assessed for variance homogeneity by both the Bartlett and Levene tests. Tukey's Honestly Statistically Different post hoc test was used to examine individual comparisons after statistical significance was observed in the ANOVA analysis. Statistical significance was established at the p=0.05 level. All data are graphically presented as mean ±standard error of the mean.

Results:

Figure 1. Image of a 1-month old male Fischer 344 rat (left) and the partially dissected hind-limb Achilles tendon (right).

Tenocyte explant cultures were monitored during growth and documented by taking light microscopy images of the culture dishes. Analysis of the cellular morphology revealed differences between the two groups of cells isolated from the Achilles tendons of juvenile and aged rats. The cells isolated from 22-month old rats were distinctively longer and wider. The

aged cells also had larger nuclear perimeters (Fig. 2). Cells from both age groups had maintained their characteristic spindle shapes, but the older cells had consistently larger features (longer, wider, and larger nuclei). Furthermore, the cellular measurements seemed to be larger in equal proportions suggesting the older cells were approximately a scaled-up version of the younger cells. Surprisingly when measured in suspension, the cells showed no significant differences in size and were always approximately 20um in diameter, (data not shown). In consideration of both cell measurements (adherent and in suspension), the older cells spread more when adhered to tissue culture plastic, despite being approximately the same size in suspension, suggesting morphological and cytoskeletal differences in vitro.

The figure below shows the explant yields of the two culture groups. The tendons from 22-month old rats consistently produced lower yields than the 1-month old rat tendons. Cells growing out of the tissue explant can be seen in the images below, featuring both aged explant culture (top-left) and juvenile explant culture (bottom-left), and are consistent with the culture yield quantification on the lower right. Note the images in the figure below are at 5X magnification and were not used to quantify morphological cellular features; additional images at 20X magnification were used to quantify morphology for each of the age groups.

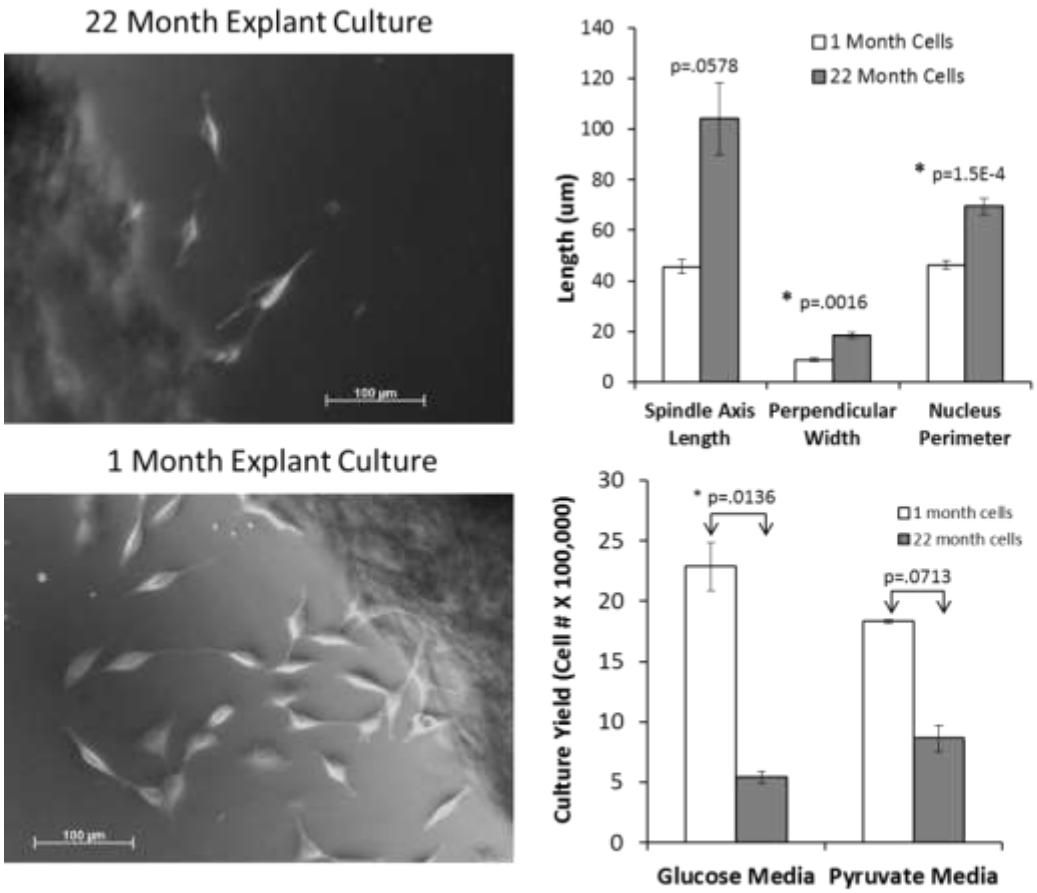

Figure 2. Images of cells growing out from explant cultures of the Achilles tendons of 22 month and 1 month rats (left). Images displaying the tissue boundary were taken 8 days after isolating the tissue and placing them in culture. The upper right bar graph displays key differences in morphological features of the spindle shaped cells. The lower right figure displays the yield (total number of cells) for each of the age groups.

The growth rate of the cultures was investigated to determine the proliferative capacity of the cells in culture. The 22-month tenocytes demonstrated more rapid growth rates over a 3 day period (Fig.3). The glucose and pyruvate supplemented DMEM is considered normal growth conditions in this study. The metabolic substrates play a significant role in the proliferation of the tendon cells, and this will be discussed later in more detail. All growth media formulations contained 10% FBS to stimulate growth.

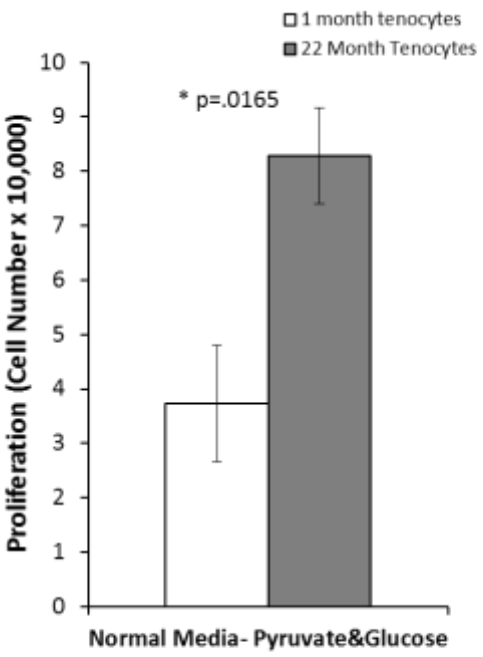

Figure 3. Cell proliferation. Cells were plated at approximately 3,000 cells per cm^2 and counts were used to determine relative proliferation after 3 days in culture.

Telomere length was investigated to characterize the age, or more accurately the replicative history, of the cells derived from the explant cultures. The two age groups showed no significant difference and had very consistent mean terminal restriction fragment lengths (Fig. 4). The positive control was obtained commercially from Roche and the digested DNA separated within the limits of the 100 bp to 20 kbp molecular weight marker.

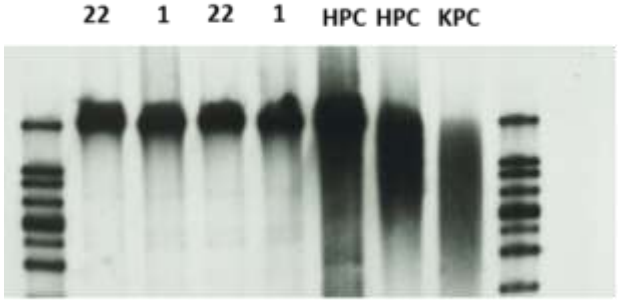

Legend

22	DNA from cells isolated from 22 month rat tendon
1	DNA from cells isolated from 1 month rat tendon
HPC	Human DNA controls (not from tendon cells)
KPC	Kit supplied control DNA

$$\frac{\sum(OD_i - Background)}{\sum(^{OD_i - Background}/_{L_i})}$$

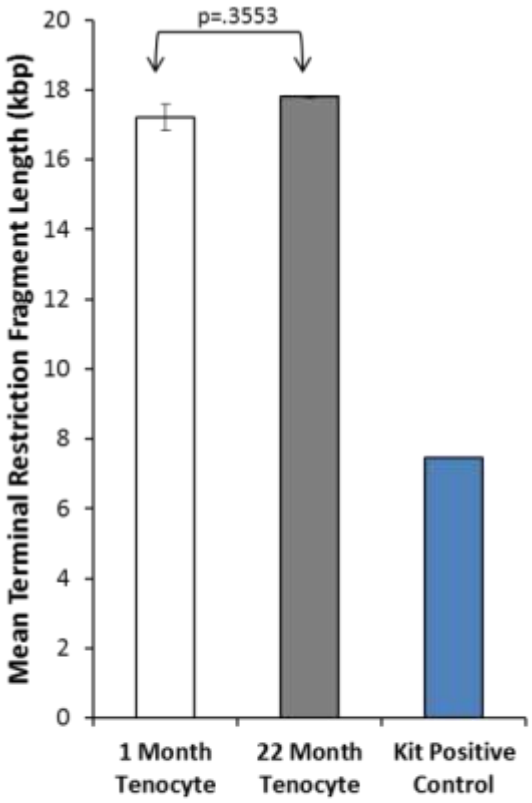

Figure 4. A representative image of a radiograph showing the separation of DNA after restriction enzyme digestion (left). The data on the right shows the mean telomere restriction fragment length (TRF). The equation used for the calculation to determine TRF is included on the left. There is no significant difference in mean telomere length between the cells isolated from the two age groups.

TEM imaging revealed stark differences in tendon fibril size and arrangement. The tendon fibrils from 1-month old rats are uniform in size as shown by the narrow range and nearly normal form of the distribution shown in the histogram of Figure 5. The fibril perimeters range from 200 to approximately 600 nm and are densely packed within the tissue. In contrast, the size of the collagen fibrils from the 22-month old rats are widely distributed. The fibril perimeter span is from about 100 nm to over 900 nm (Fig. 5). The distribution of the fibrils from the 1-month old rats is monophasic while the distribution of the fibrils from the 22-month old rats is biphasic with both a high and a low peak in fibril perimeter. In addition, a noticeably

large amount of space exists between parallel fibers, and as a result the density of the fibrils varies widely throughout the tissue of the 22-month old rats.

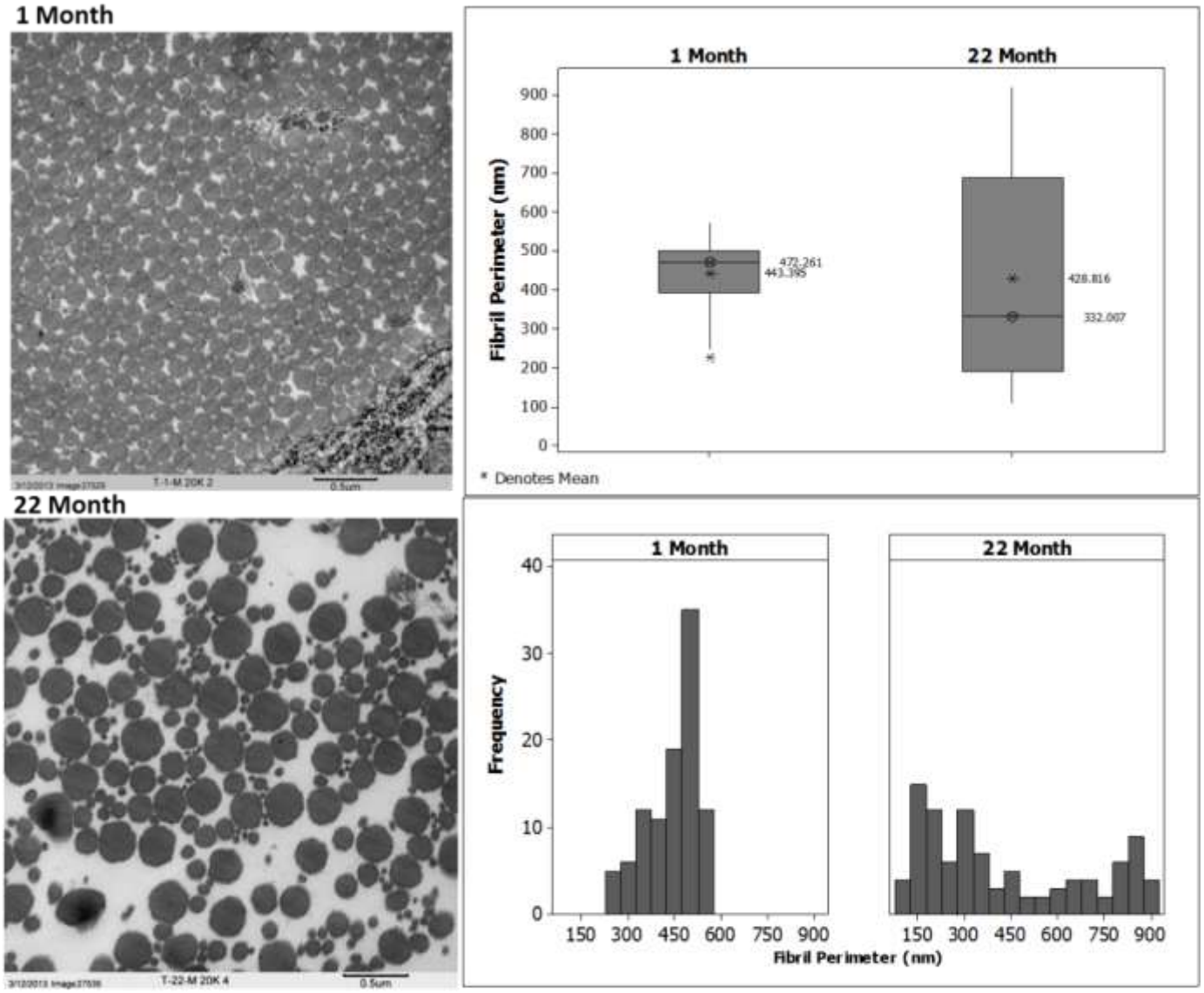

Figure 5. Transmission electron micrograph images representative of tendon samples at 20,000X magnification. The graphs on the right show clear differences in the distribution of fibril perimeters between the two age groups. Boxplot (top right) and histogram (bottom right).

Cell counts indicating the cellular density of the tissue demonstrated a sharp decrease in cellular content for the 22-month rat tendon (Fig. 6). While observing the cellular density of the longitudinal sections via normal light microscopy cartilaginous tissue was identified near the tendon midsubstance (Fig. 7). The cartilaginous tissue is indicated by chondrocyte-like cells and

a lack of fibrillar organization in the surrounding area. The chondrocyte-like cells are spherical and lack cytoplasmic as well as nuclear elongation. The cells appear randomly situated in a mass of unorganized tissue as opposed to lining the fibril striations as is clearly depicted in the 1-month healthy tendon. A subtle transition can even be identified from normal tendon with the characteristic longitudinal fiber striation to the cartilaginous tissue, which lacks visible organization (Fig. 7 top-right image).

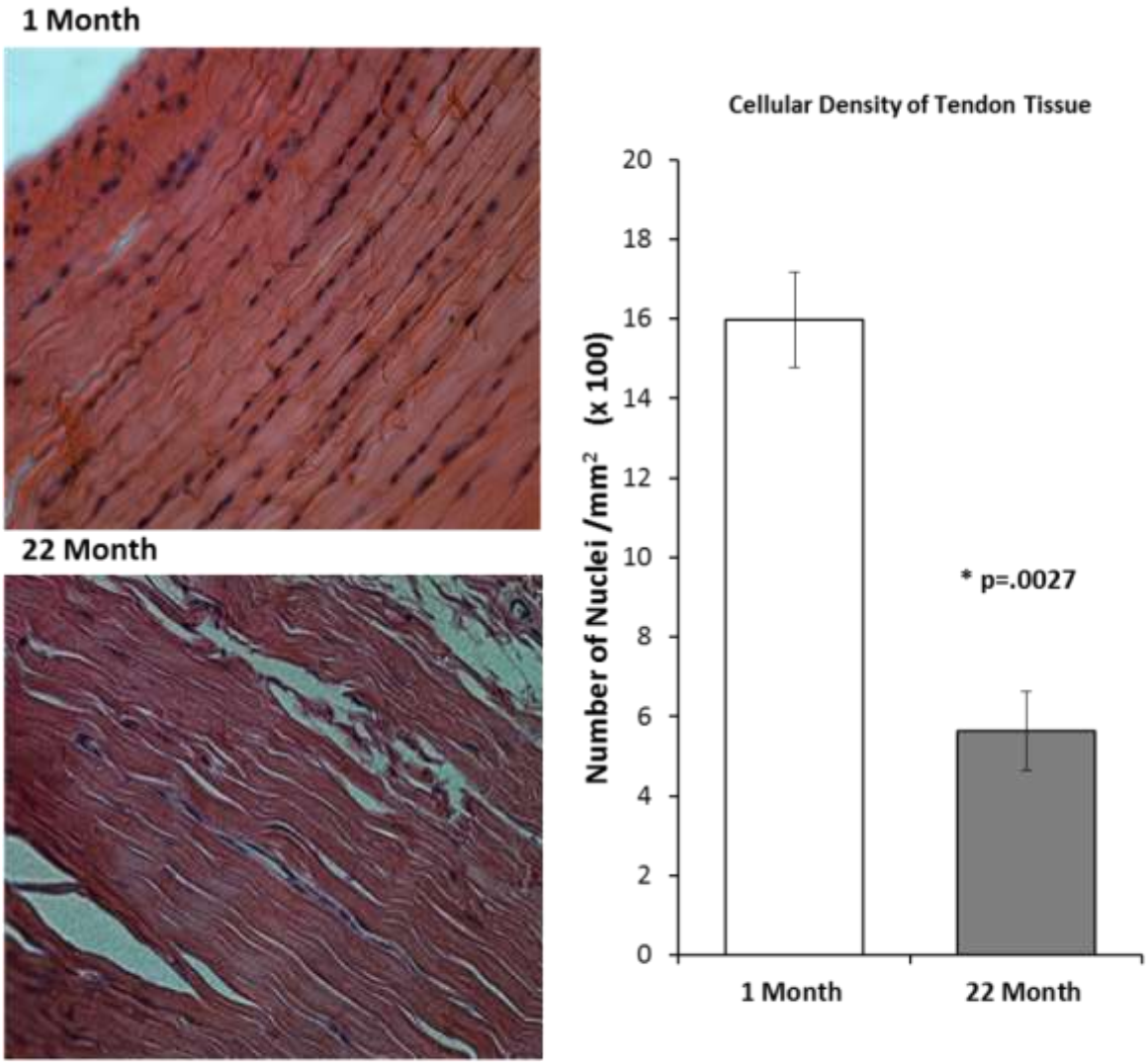

Figure 6. Representative images of longitudinal sections of Achilles tendons isolated from 1 month and 22 month rats (left). Bar graph on the right shows quantification of the number of stained nuclei per mm² of tissue.

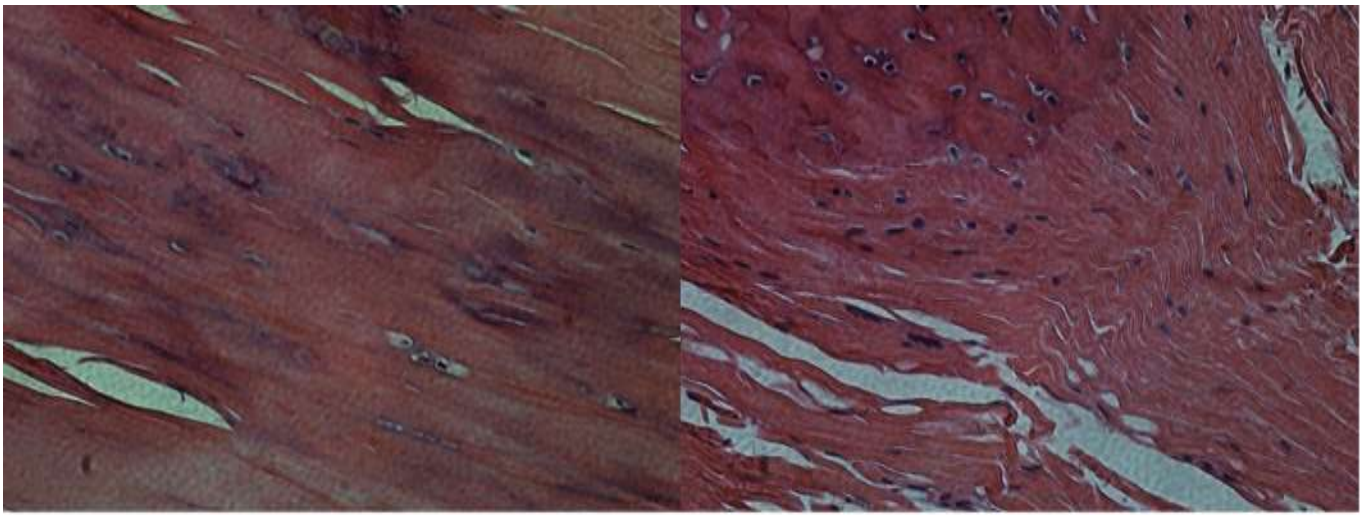

Figure 7. Longitudinal sections of excised Achilles tendon from 22-month old rats. Both images were taken at 40x magnification and display two distinct sites that contain spherical cells within the tissue. The tissue surrounding the chondrocyte-like cells lacks definitive fibrillar organization. The approximate location of the tissue from which the images were obtained is represented diagrammatically (bottom left).

Discussion:

The results in part 1 provide a detailed characterization of both the tendon explant cultures and the tissue from which the cells originate. The characterization indicates many similarities between the aged rat Achilles tendon and the human tendinopathic phenotype, which is well documented in the literature. Part 1 serves as a foundation for clinical comparison and validates the similarities in phenotype between cells in aging rat tendon and degenerative human tendon.

The Achilles tendons of aged rats demonstrate significant tissue-level changes from the juvenile tendons including architectural and cellular incongruities. The most drastic of these changes was demonstrated by the TEM examination of collagen fibrils. The organization and

regulation of fibrillogenesis appears to be highly dysfunctional in tendon from the older rats. The distribution of tendon fibrils abnormally spans a spectrum of perimeters that exceed the upper and lower limits of the normal fibril distribution in the younger animal. The regular and consistent distribution of normal fibers is displayed in the younger, yet mature, 1-month old rat tissue specimen. Additionally, the irregular spacing between the collagen fibrils is easily viewed in cross-section. It is important to note that fibrils do not span the length of the entire tendon and do naturally taper. The tapering of fibers causes some minor variation in fibril diameter that can be seen in the tendon sections of the 1-month old rat; however, this level of fibril variation is minimal compared to the apparent dysregulation of collagen fibrils in tendon of the 22-month old rats. Very similar age-related collagen changes in fibril diameter and organization have been documented in aged human Achilles tendon [14]. Additionally, the impact of collagen-level dysfunction has been implicated in leading to biomechanical insufficiencies consistent with tendon degeneration [12]. Specifically, an increase in large diameter fibrils in the tendon results in an increase in the maximal tensile strength of the tendon, but also reduces the elasticity of the tissue, which is predominantly attributed to small diameter fibrils. The decrease in elasticity leaves the tendon more susceptible to crack propagation, a mechanism of tendon rupture [15].

The histological data presented here displays two strong indicators of age-related degeneration. The first is abnormal, variable cell density and the second is the presence of heterogeneous tissue within the tendon. The presence of cartilage-like tissue is indicated by a lack of parallel fibrils and the manifestation of chondrocyte-like cells within the disorganized mass. Chondroid metaplasia has been histologically identified in tissue biopsies of Achilles

tendinopathy in humans [16]. A few studies have raised the possibility that native tendon cells may be able to undergo chondrogenic differentiation, and there is evidence for load-dependent regulation of cartilaginous phenotypes within the tendon[17], [18]. Despite the cellular origin or mechanical contribution to the chondroid heterogeneity, the presence of this tendinopathic marker validates degenerative tissue changes in the aged rat model used in this study.

Characterization of the tendon cell cultures, generally referred to as tenocytes despite the possibility of multiple cell types as a result of the primary explant culture technique used to harvest the cells, identified modest cellular differences. Not surprisingly, the tendon cell culture from the 22-month rat Achilles tendon had lower yields in terms of cell number. The low yields and lower cellularity are consistent, but it is also possible that there are other contributing factors to the low yields such as decreased proliferative capacity or restricted cellular migration through degenerated extracellular matrix. To partially address the possibility of reduced proliferation, the cells were plated at roughly 3,000 cells/cm^2 and growth was monitored and measured at a 3 day endpoint. The results depict a higher growth rate for the aged cells. The cells from the aged animals do not show a deficiency in growth rate when grown in cell culture.

Telomeres play a critical role in maintaining the genetic content of eukaryotic cells. The telomere length is an indicator of replicative history of the cells and was quantified to investigate the tendon cells isolated from the two different age groups. The data indicates no significant difference in telomere length between cells from the 1-month old rats and 22-month old rats. In congruence with the proliferative data, the telomere length data suggests that aged cells are not less active in maintaining tissue homeostasis due to lack of fundamental proliferative capacity or replicative exhaustion of telomeres. Moreover, our data agrees with a

previous report that older tendon cells isolated from aged mice did not contain higher levels of the senescent marker β-galactosidase, but instead suggested a phenotypic shift rather than the onset of cellular senescence[19]. This characterization of tenocyte cell culture proliferation implies that some cellular dysfunction exists in vivo despite the demonstrated capacity and essential cellular machinery for division in vitro.

Part 2: Tendon Cell Metabolism: An Investigation of Glycolysis and Mitochondrial Function

Introduction:

Although the pathogenesis of tendinopathy is unclear, aging fundamentally changes tendon structure and function in a degenerative manner. Tendon degeneration is a widespread clinical concern, which takes on many forms and generally progresses with aging [20]. The focus of part 2 will be on energy metabolism in relation to cellular dysfunction.

Despite a relatively low metabolic rate, tenocytes produce energy by both aerobic and anaerobic mechanisms, including glycolysis, oxidative phosphorylation, and the pentose phosphate pathway [10]. One key age-related characteristic that has been implicated by microscopic examination of degenerative tendon is a the divergence of native tendon cells to a glycolytic phenotype[12], [21]. The lack of defined organelle structures necessary to fundamental metabolism has been touched upon with a specific focus on the golgi, endoplasmic reticulum, and mitochondria[21]. The number of mitochondria is decreased with aging, and aged cells exhibit a characteristic buildup of glycogen, lysosomes, and lipofuscin [12]. It was implicated that the citric acid cycle is shut down with a complete shift to anaerobic metabolism with advanced age. These observations imply a characteristic shift in the metabolic machinery of aged tendon cells. The metabolic phenotype, with regard to energy production, of aged tendon cells has not been studied in depth, yet there is significant literature that indirectly suggests a relationship between tenocyte metabolism and tendon degeneration.

There are a number of metabolic diseases, including diabetes, obesity, hypercholesterolemia, hyperuricemia, and glucose-6-phophatase deficiency, that are characterized by a surprisingly high incidence of tendon degeneration and concomitant clinical

complication. In some cases such as diabetes, metabolic byproducts associated with the primary disease condition are considered to have deleterious effects on the mechanical function of the tendons [22]. These diseases are multifactorial and exhibit an abundance of systemic pathological consequences, but are generally characterized by poor systemic regulation of energetic substrates such as glucose. Although the pathogenesis of tendinopathy is not limited to the metabolic basis of the disease, the consistent occurrence of tendinopathy warrants further investigation.

Mitochondria also represent an intriguing metabolic target that may play a role in age-related tendinopathy. Mitochondria are the fundamental biochemical machinery responsible for oxidative phosphorylation and ATP production[23]. It was previously reported that mitochondria lack definitive structure in aged tendon and the native tendon cells may be more glycolytic, which suggests age-related dysfunction and perhaps an adaptive shift in response to dysfunction [21]. ATP has also been shown to modulate the load-response of native tendon cells[24]. In addition, mitochondria, as a major source of ATP, may also play a role in tendon load response. The importance of oxidative stress and the associated molecular species, such as nitric oxide ($NO^{\cdot}$), in tendon healing has been suggested in the literature[25], [26]. Mitochondria are a major metabolic contributor to reactive nitrogen species (RNS) and reactive oxygen species (ROS) in most cell types [23]. Lastly, there is a large body of work debating the possibility of mitochondrial roles in aging. Mitochondria represent a complex metabolic entity that may play an important role in tendon cell function.

In part 2 of this investigation, we aimed to determine metabolic deficiencies, or more simply metabolic discrepancies between the two age groups of rat Achilles tendon cells. We

aimed to quantify glycolytic function and oxidative function in the tendon cells isolated from both 1-month and 22-month old rats. In order to further investigate metabolic divergence, we introduced variable media conditions to limit the availability of glucose and determine the impact of glucose deprivation on the metabolic response of the tendon cells. This metabolic assessment of the two age groups served to identify age-dependent divergence and elucidate the role of metabolic dysfunction in tendon pathology.

Methods:

Proliferation in substrate-specific media

Proliferation was assessed under three different media conditions. High Glucose (25mM), Pyruvate (5mM) and Glucose + Pyruvate media were assessed to determine the growth response of the tendon cells. Cell numbers were quantified by cell counting methods, as previously described in Part 1.

Lactic Acid Quantification

Lactate quantification was performed according to the manufacturer's instructions (Lactate Assay Kit-Sigma). $2x10^5$ cells were homogenized in kit buffer (counted using the Scepter cell counter immediately before sample preparation), vortexed, and then spun down at 14,000xg in 10 kDa molecular weight cutoff spin filters (Millipore) for 20 minutes to remove cell-derived lactate dehydrogenase. A standard curve was produced using the lactate standard provided with the kit. A serial dilution of sample volumes was tested to determine the optimal sample volume that fell within the linear range of the standard curve. Samples were loaded in Costar clear 96-well plates and enzyme mix was added to initiate the colorimetric reaction. The plates were shielded from light and incubated at room temperature for 30 minutes. Absorbance was

measured at 570 nm. Background was measured in duplicates an subtracted from all experimental groups.

Lactate Dehydrogenase Activity

Lactate dehydrogenase enzyme activity was quantified colorimetrically by the LDH assay kit (Sigma) according the manufacturer's instructions. Cells in culture were rinsed with warm (37°) PBS and trypsinized from culture plates. Approximately $2x10^5$ cells were used for each sample, measured using the Scepter cell counter immediately before sample preparation. The cells were homogenized in assay buffer provided by the kit. Serial dilutions of the homogenized cell extracts were tested to determine the appropriate sample volume (2-50 µL) for reading within the linear range of the standard curve. The assay was performed in quadruplicates and a standard curve was constructed based on the NADH standard provided in the kit. After the substrate was added, colorimetric measurements were taken every five minutes at 450 nm with shaking before each measurement for a total of 25 minutes. Background measurements were performed in duplicates and subtracted across all experimental groups.

Mitochondrial Membrane Staining (CMXRos)

A mixture of Hoechst 33342 and CMXRos dyes (Molecular Probes) were used to quantify nuclear and mitochondrial content of cells for each age group. Cells were plated at approximately 15,000 cells/cm^2 in black 96-well plates with clear bottoms (CoStar). The plating was done in a side-by-side manner so that all experimental groups were represented on a single plate to ensure there was no effect of instrument bias. Cells were allowed to adhere over a period of 6-8 hours, which is approximately one-third of the doubling time for the fastest growing tenocytes, to allow for cell adhesion, but to minimize duplication. Cell adhesion and density in the well were checked by viewing each well at 10X magnification under an inverted

light microscope. Both dyes were diluted with PBS to achieve final concentrations (Hoechst 33342: 1.62 µM & CMXRos: 20 nM). Cells were incubated for 15 minutes at 37°C. The loading solution was removed and the wells were washed 3 times with PBS. Normal growth media (5 mM pyruvate and 25 mM glucose) was added to each well and fluorescence measured using the PHERAstar FS microplate reader. Background fluorescence (cells + media solution without fluorescence dye) was measured in duplicates and was subtracted from each of the experimental groups of interest. Blank wells (without cells) were treated with the same loading solution and wash steps then measured to verify any residual fluorescence.

Mitochondrial Membrane Potential (JC-1)

JC-1 dye (Molecular Probes) was applied in an analogous manner to the mitochondrial staining procedure above. Cells were plated at approximately 15,000 cells/cm^2 in black 96-well clear-bottomed plates. The cells were plated such that all of the experimental groups were tested side-by-side on the same plate to minimize variability between measurements of different plates. The stock dye was diluted with PBS to a final concentration of 0.3 µg/mL. The cells were then incubated at 37°C for 1 hour. The loading solution was removed and the cells were washed 3 times with warm (37°) PBS. Normal culture media was added to the cells and fluorescence measured using a PHERAstar FS microplate reader. JC-1 fluoresces at two wavelengths, depending on the aggregation of the monomer form of the dye (discussed in detail in the results), green fluorescence was measured first at 485 nm/ 525nm and then red fluorescence was measured at 520 nm / 595 nm (excitation/emission). Background fluorescence (cells + culture media without fluorescence dye) was measured in duplicates and subtracted from the raw data across all of the experimental groups. Blank wells (without cells) were also quantified in duplicate after applying identical incubation and wash steps to

determine the effect of any residual loading buffer. Cells were plated no more than 6-8 hours before measuring fluorescence to allow cell adhesion, but to minimize replication.

Western Blot

Total protein was extracted from $1x10^6$ passage 3 tendon cells. Briefly, cells were washed with 1X PBS and trypsinized. After trypsinization the cell pellet was collected and 400 µl RIPA (20 mM Tris-HCl (pH 7.5), 150 mM NaCl, 1 mM Na2EDTA, 1 mM EGTA,1% NP-40, 1% sodium deoxycholate, 2.5 mM sodium pyrophosphate, 1 mM beta-glycerophosphate, 1 mM Na3VO4, 1 µg/ml leupeptin) buffer was added for lysis. The lysis suspension was vortexed 3 times for 10 seconds each and sonicated twice for 30 seconds in an ice bath.

The extract was centrifuged for 10 minutes at 14,000 x g at 4°C. The supernatant was collected and protein concentration was measured using the Bradford method (Bio-Rad).

Immunoblotting was performed using the Mini PROTEAN 3 system (Biorad). Samples of 12.5 µg total protein were separated on 15% tris-glycine PAGE gel. Electrophoresis was carried out at a constant 85 volts for 2.5 hours. Samples were then transferred onto a 0.2 µm nitrocellulose membrane in 20% methanol transfer buffer for 90 minutes. Nonspecific binding was blocked with 3.5% non-fat milk in TBS-T for 1 hr at 37°C. The membrane was incubated with primary antibody at a 1:2000 COX IV (Abcam) or GAPDH 1:2000 (CellSignaling) dilution. Secondary antibody (horseradish peroxidase-anti-mouse antibody, and horseradish peroxidase-anti-rabbit antibody) (Amersham Bioscience) was at a 1:2000 dilution. The incubation of both primary and secondary antibodies was done at 37°C for 1 h with 3 X 10 min washing (TBS-T) in between. ECLplus (Amersham Bioscience) reagent was used for detection.

ATP Quantification

Tenocytes of both age groups were seeded in black, clear-bottomed 96-well plates at approximately 30,000 cells/cm^2. Again cells from each experimental group of interest were plated on the same plate. The cells were allowed to adhere for no more than 8 hours to minimize cell duplication. Cell adhesion and cellular density was confirmed by light microscopy (10X magnification) just prior to the assay. A luciferin-based luminescent assay (Promega- Cell Titre-Glo) was used to detect the relative quantities of ATP. The cells were rinsed several times with PBS before any of the kit reagents were added. A PHERAstar FS microplate reader was used to luminescence intensity data. The data was recorded every minute for 10 to 20 minutes to ensure luminescence stability. Background luminescence (cells in PBS) was measured in duplicate wells and subtracted across all experimental groups. Blank wells (without cells) were also measured for residual luminescence, but this luminescence was negligible in comparison to the wells with cells.

Broad Spectrum ROS Quantitation

CM-H_2DCDFDA (Molecular Probes) was used as a general indicator of oxidative stress. Cells were plated at 30,000 cells per cm^2 to yield a confluent monolayer and allowed to adhere for no more than 8 hours. As mentioned previously 8 hours is approximately one-third of the doubling rate of the fastest growing tenocytes; eight hours allowed for complete adhesion and minimized the duplication of the plated cells. Adhesion and cellular density was qualitatively examined at 10x magnification on an inverted light microscope. The dye solution was prepared in prewarmed PBS (37°C at 10uM final concentration). The cells were rinsed with PBS before the loading solution was added. The plates were incubated for 30 minutes at 37°C, and then rinsed with PBS. Fluorescence was measured at 495nm/520nm (excitation/emission) using the same PHERAstar microplate reader mentioned above. The measurement was continued over

time (10-20 minutes) to verify fluorescence stability. As mentioned in earlier fluorescence methods both blank wells (without cells) and background fluorescence was measured and then subtracted from the raw data.

Oxygen Consumption

Cellular oxygen consumption was tested using the Seahorse Biosciences XF24Flux Analyzer system. Cells were plated at approximately 75,000 cells/ cm^2 ($0.3cm^2$/well) and allowed to adhere overnight in culture media. After conditioning the cells in either glucose- or pyruvate-supplemented media, the culture media was replaced with 1mM pyruvate-supplemented non-bicarbonate buffered media with 25mM HEPES to prevent acidification (termed running media) for all groups to ensure that substrate was not a limiting factor in determining the oxygen consumption ability of the cells. The groups were plated in quintuplicates and each well was normalized by the total protein content for that well (protein was measured immediately after carrying out the oxygen consumption measurements). Normalizing by the total protein eliminated the potential effect of intra-well variability in cell density. A series of three measurements were taken at approximately 3.5 minute intervals after the addition of each pharmacological inhibitor. The three measurements were always consistent and were averaged; the averages are displayed in Figure 16. First FCCP sensitivity was determined by sequential injections of 750uM, 100nM and 1uM, or 500nM and 2uM FCCP. After the FCCP optimization was carried out, the oxygen consumption was measured during a mitochondrial stress test (Figure 16) Pharmacological agents were injected in the following order during the stress test: 1ug/mL oligomycin (Sigma), 2uM FCCP (optimized), 1uM rotenone. This precise order for the addition of pharmacological agents is necessary for the isolation / uncoupling of

mitochondrial processes of cellular. More information on the pharmacological impact of these substances is provided in the discussion below.

Results:

The growth data displays a hyper-proliferative response of the tendon cells from 22-month old rats in the presence of glucose compared to the cells from 1-month old rats (Fig. 8). The one month tendon cells did not demonstrate a glucose-dependent growth pattern, but instead maintained consistent proliferation under all media conditions. Interestingly when the aged tendon cells were starved of glucose and allowed only to use pyruvate as a substrate for energy production, proliferation was limited to rates equal to that of the 1-month age group.

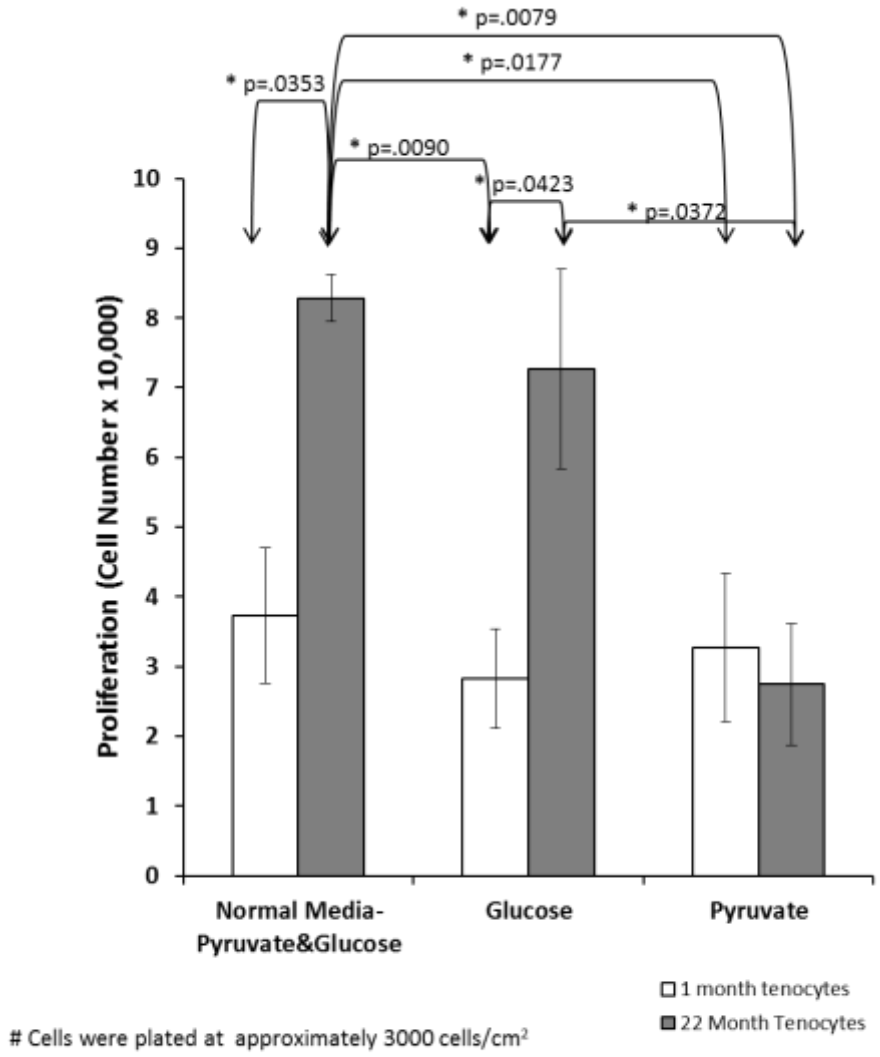

Figure 8. The effect of glucose supplementation on the proliferation of cells from each age group. The data shows cell counts after 72 hours in culture.

In identical media conditions, supplemented with both glucose and pyruvate, the lactate concentration and lactate dehydrogenase activity of the cells isolated from 22-month old rats was significantly increased (Fig. 9). This data is strong evidence of the activation of glycolytic metabolism in aged cells. Glucose was then removed from the media to determine the effect on glycolytic activation. Cells from the 22-month rats responded to glucose starvation by reducing the activity of LDH (Fig. 10).

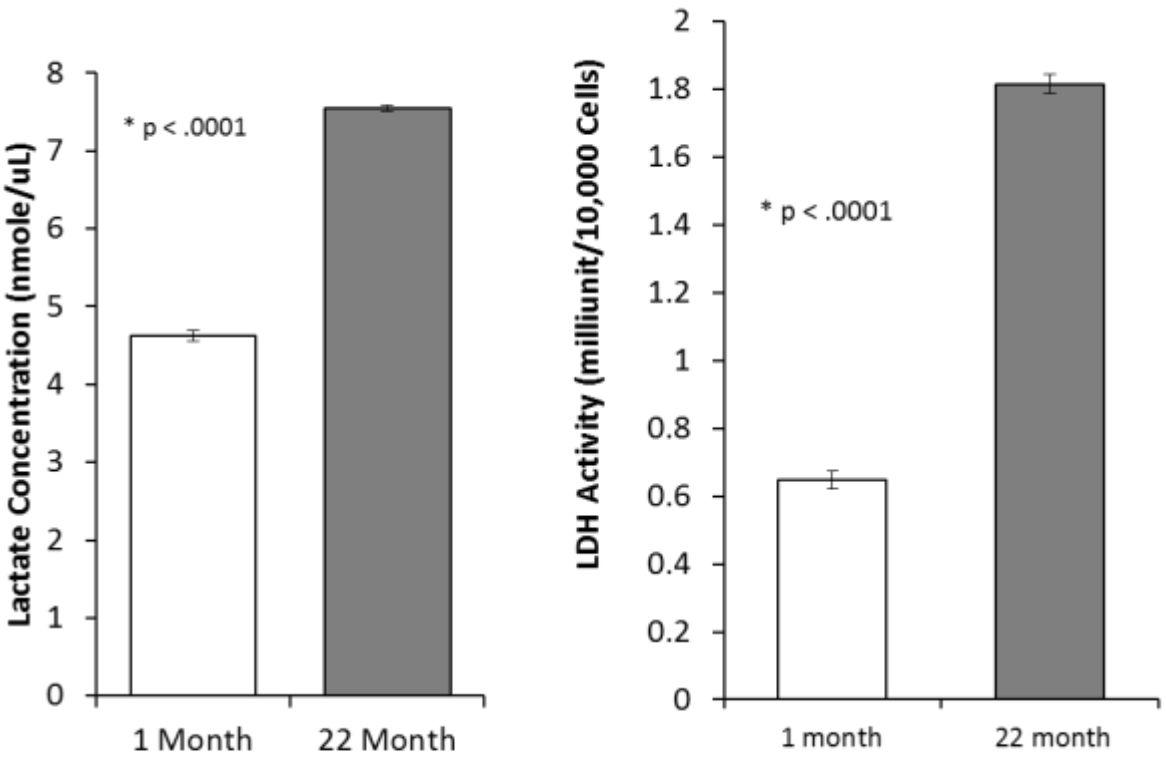

Figure 9. Lactate concentration (left) in extracts of cells from the two age groups, and, lactate dehydrogenase activity (right) of the same cell extracts. Significant increases were observed for both lactate concentration and LDH activity between the cells isolated from older rats and those isolated from juvenile rats.

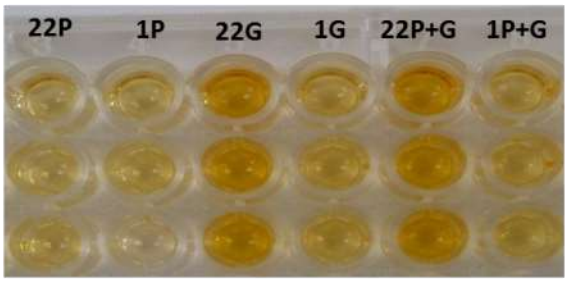

Figure 10. Effect of glucose on lactate dehydrogenase activity. The image above is representative of the LDH activity assay. Data in the figure on the right shows that glucose increases lactate dehydrogenase activity in the cells isolated from 22 month old rats. The change in LDH activity as a result of treating the cells from 1 month old rats with glucose is not statistically significant.

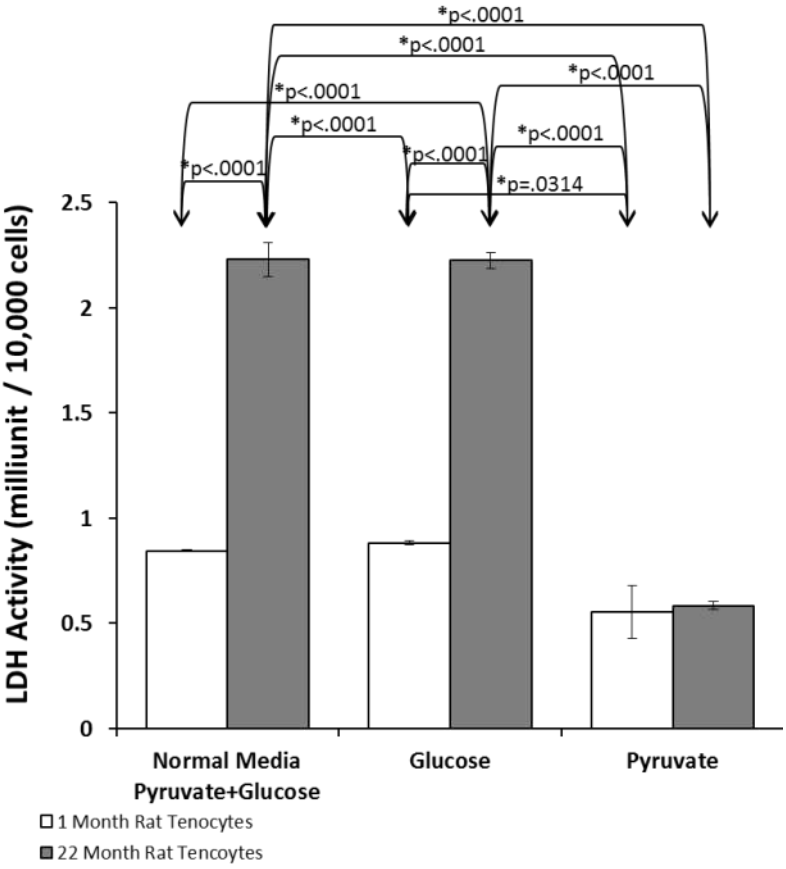

Mitochondrial staining using both JC-1 and CMXRos mitochondrial membrane targeted probes show minor, but consistent decreases in fluorescence intensity in the 22-month tendon cells. The images of the CMXRos fluorescence show a more diffuse scattering of fluorescence for the aged cells (Fig. 11). The nuclei are stained with DAPI to normalize the mitochondrial labeling by nuclear content. In the JC-1 staining experiments, the fluorescence intensity is represented by the ratio of the aggregate to monomer fluorescence. Again the data indicates a lower level of aggregate formation corresponding to membrane depolarization (Fig. 12). The physiological significance of the staining is difficult to determine based on only minor indications of depolarization in the aged tendon cells.

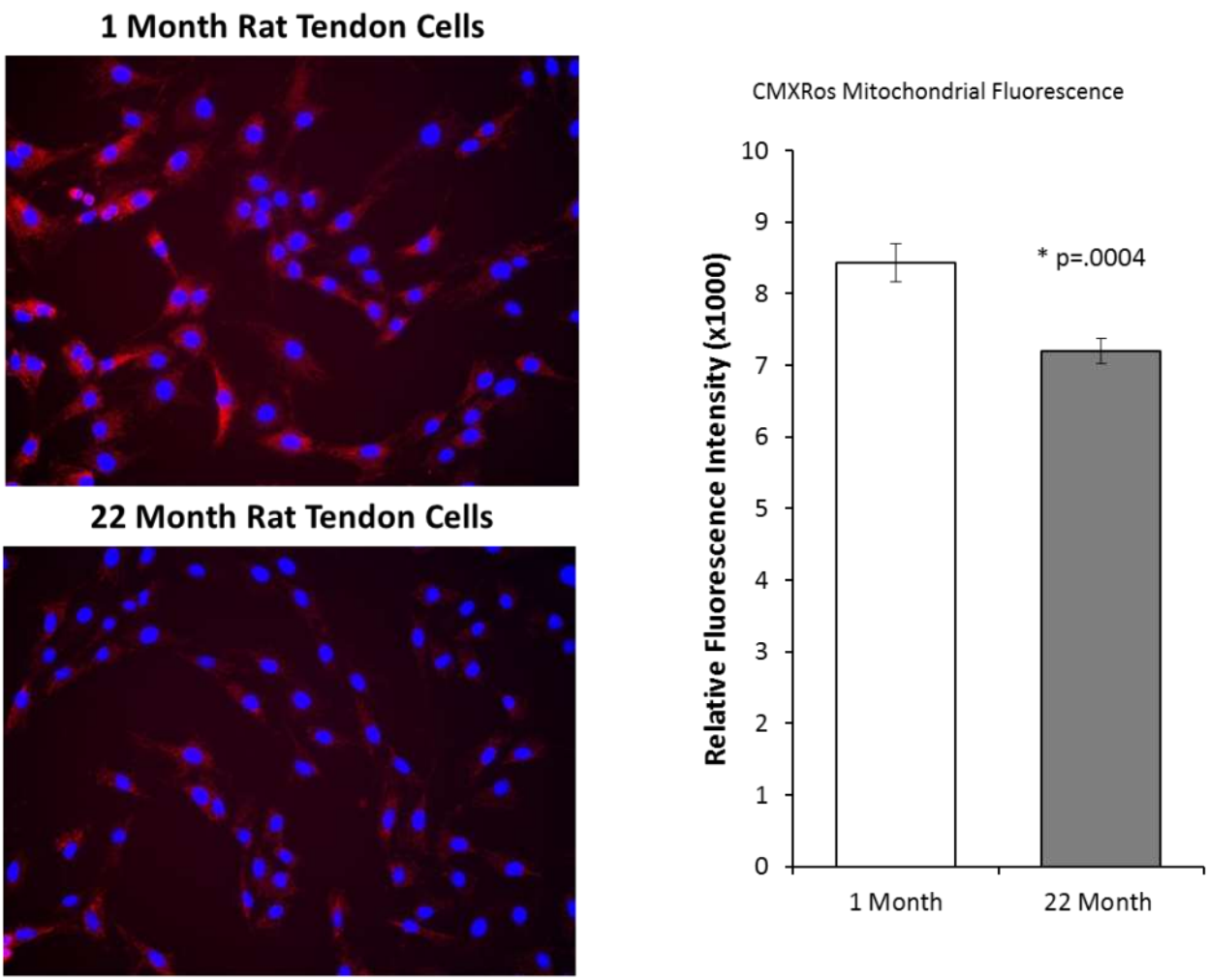

Figure 11. CMXRos, a rosamine based mitochondrial dye, was used to assess the mitochondrial content and membrane potential of tendon cells isolated from 22 month and 1 month F344 rats. Representative images of the fluorescence (nuclei stained with Hoechst 33342) at 20x magnification are shown on the left. Data was captured using a 96-well fluorescence plate reader. The results demonstrate a relatively small (15%) decrease in fluorescent intensity indicating mitochondrial membrane depolarization of the cells isolated from the older rats.

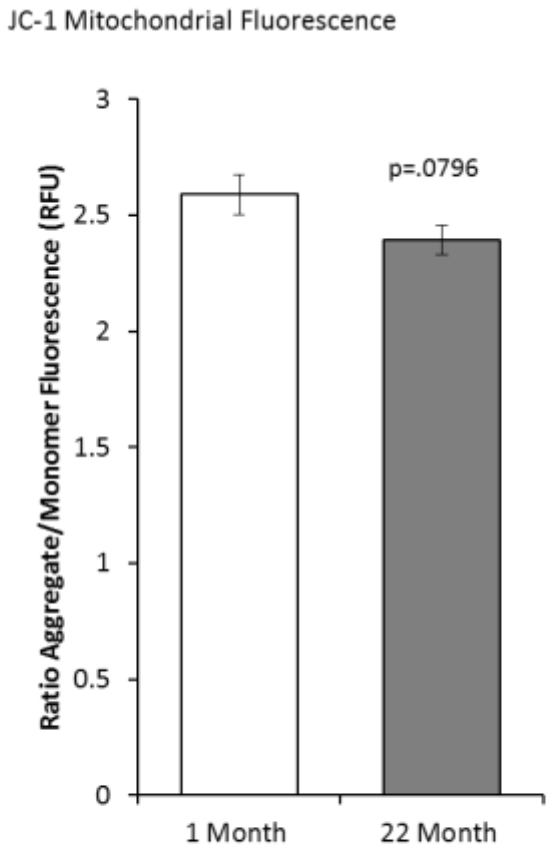

Figure 12. JC-1 staining for mitochondrial membrane potential indicated no significant differences between the cells isolated from 22 month rats and cells isolated from 1 month rats, but indicated slight membrane depolarization for the cells from the older rat.

Western blot analysis of cytochrome c oxidase subunit IV indicated similar levels of protein for the 22-month and 1-month tendon cells grown in glucose media conditions (Fig. 13). When the cells were starved of glucose by supplementing the media only with pyruvate, the 22-month tendon cells displayed higher protein levels suggesting an increase in the electron transport machinery necessary for ATP production and simultaneous oxygen consumption. The 1-month tendon cells demonstrated consistent levels of COXIV protein despite glucose deprivation.

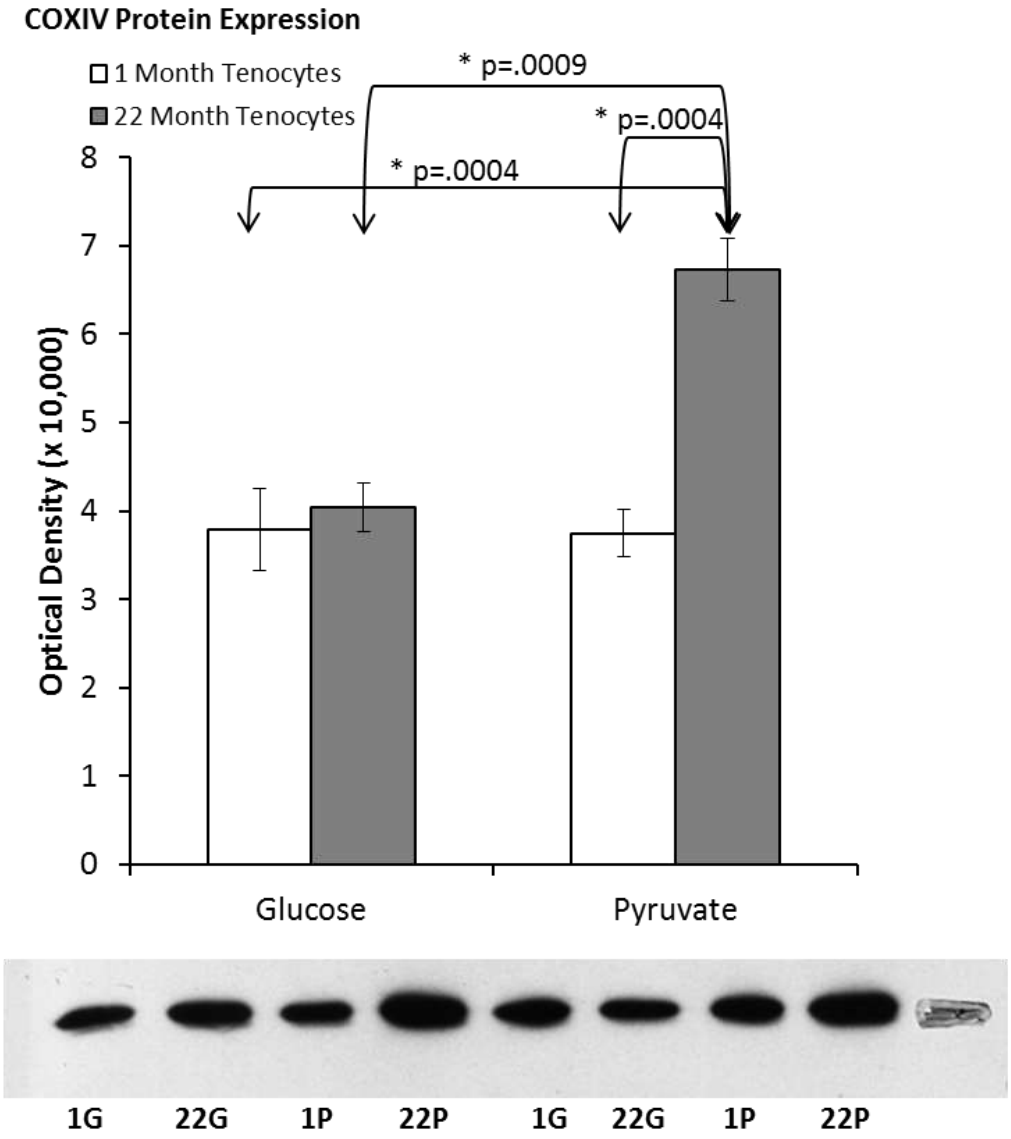

Figure 13. Effect of glucose deprivation on COXIV protein. Quantification of COXIV from a western blot reveals a significant change in COXIV protein in cells from the 22 month rat tendons when the cells are subjected to glucose deprivation.

ROS quantification revealed a significant decrease in reactive oxygen species for the aged tendon cells (Fig. 14). The juvenile tendon cells repeatedly displayed signs of increased oxidative metabolism compared to the 22-month tendon cells.

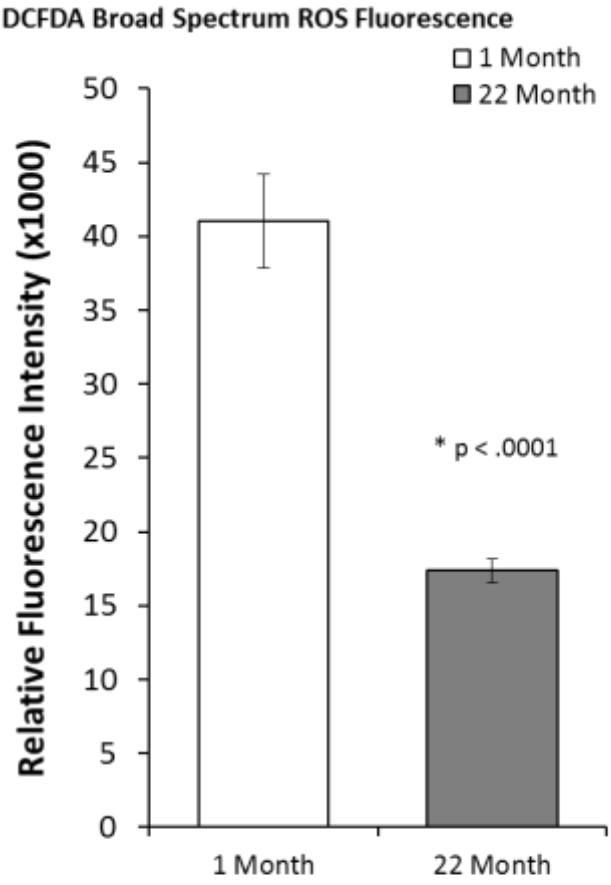

Figure 14. Broad spectrum fluorescence for reactive oxygen species (DCFDA). Cells isolated from 22 month animals displayed a 58% decrease in fluorescence intensity over the cells isolated from 1 month old rats.

ATP quantification by luciferase-luciferin luminescence indicated only small differences in ATP levels. The data indicates that ATP production was not significantly affected by aging (Fig. 15). The absence of specific media conditions indicates that the culture media supplemented with both pyruvate and glucose was chosen to allow the cells to freely choose their preferred substrate for ATP production.

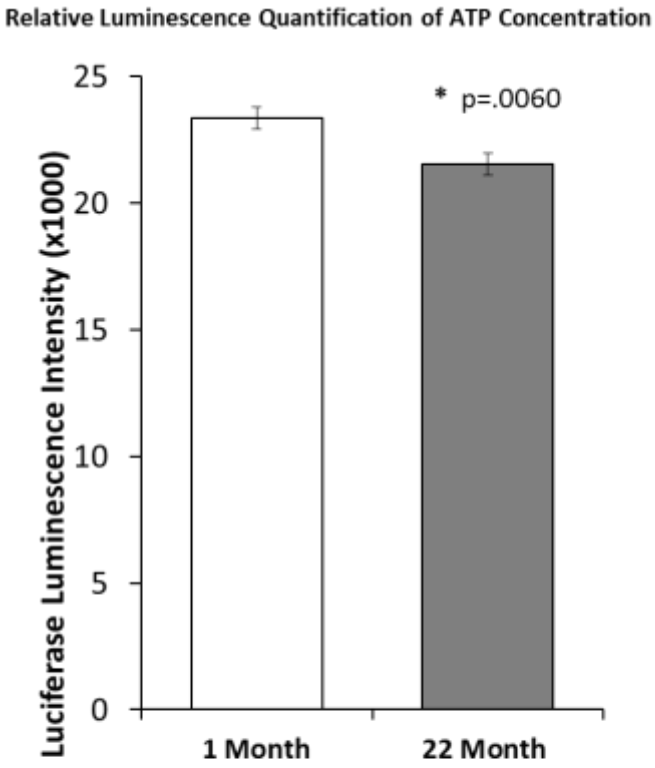

Cells plated at 30,000 cells/cm²

Figure 15. ATP was quantified using a luciferase-based luminescence assay. The results indicate very similar levels of ATP despite a small, but statistically significant decrease, of 8%, in the ATP-dependent luminescence of the cells isolated from 22 month rats.

The oxygen consumption data displayed in figure 16 reveal considerable differences in the baseline, before pharmacological inhibition, oxygen consumption rates. Interestingly, the oxygen consumption of the older cells is significantly higher than the oxygen consumption of the juvenile cells in glucose-supplemented culture media. Aged and juvenile tendon cells demonstrate divergent oxygen consumption responses to glucose deprivation (Fig.16). When cultured in glucose-free media, the oxygen consumption of the juvenile cells increases significantly. In contrast, the oxygen consumption of the older cells decreases significantly after culture in glucose-free media. This juxtaposition, between the age groups, in response to

glucose deprivation is consistent under all conditions of mitochondria inhibition. Perhaps the most striking effect is revealed after FCCP addition. The maximal oxygen consumption rates, revealed by the uncoupling of the electron transport chain and ATP synthase by FCCP, are largely dependent on the presence of glucose in the culture media. Again, the presence of pyruvate alone enhances the maximal oxygen consumption of the juvenile cells while reducing the maximal oxygen consumption of the older cells.

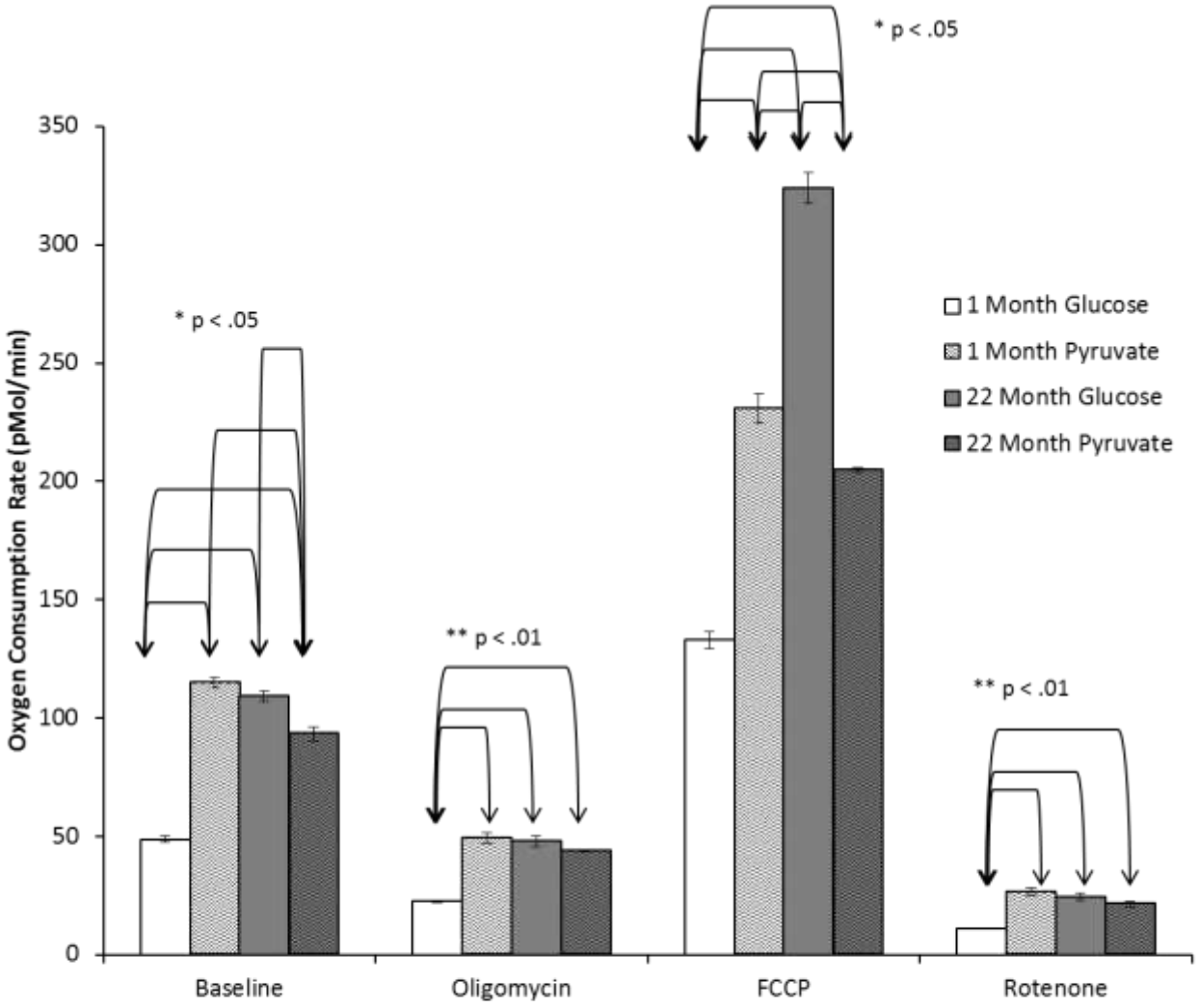

** All OCR values are normalized by total protein

Figure 16. Oxygen consumption rates of cells isolated from 1-month and 22-month old rats displayed very different results. The consumption values for each well were normalized by their respective protein content and the replicates were averaged. Normalizing by total protein mitigates any intra-well variability in cell density. There are clear differences in baseline oxygen consumption between the two age groups. The older group exhibits higher baseline oxygen consumption when grown in glucose-supplemented culture media. The age groups show divergent responses to glucose deprivation. Pyruvate growth media increases the oxygen consumption of the juvenile cells while it decreases the oxygen consumption of the older cells. This divergent response to glucose deprivation is consistent across all pharmacological treatments.

Discussion:

Aged tendon cells demonstrated enhanced glycolytic activity. The aged cells showed a strong preference for glucose-supplemented media and were not able to sustain the same level of proliferation in media supplemented with pyruvate alone. Furthermore, lactate

dehydrogenase (LDH) activity and lactate concentration were significantly increased when the cells were grown in normal culture media, containing both glucose and pyruvate. The presence of both pyruvate and glucose allows aerobic and anaerobic ATP production to occur independently; thus allowing the cells to choose between substrates. In the absence of glucose, LDH activity returned to levels comparable to the 1-month tendon cells. Surprisingly, under all media conditions the juvenile tendon cells maintained stable levels of LDH activity. The glucose-dependent increase in proliferation, LDH activity, and lactate concentration suggest the older cells depend on anaerobic glycolysis as a key mechanism for energy production. In contrast to the glucose-dependency displayed by the older cells, the juvenile cells show no response to glucose deprivation and demonstrate a robust phenotype that is capable of adapting to changes in glucose availability. It should be noted that smaller, but still substantial, levels of lactate and LDH activity were demonstrated in the extracts of the juvenile cells, implicating that anaerobic glycolysis is active, but probably to a lesser extent.

Lactate dehydrogenase is a tetrameric enzyme capable of interconverting pyruvate and lactate [27]. In the assay described above, the reducing activity in converting NAD+ to NADH was established based on spectrophotometric quantification. The reducing activity is an indicator of the ability of the enzyme to produce pyruvate from lactate stores after accumulating oxygen debt due to anaerobic metabolism [27]. The combination of high lactate concentration and increased LDH activity may suggest that the accumulation of lactate is driving the reaction toward the production of pyruvate, but it is not possible to determine such specific substrate interactions given the complexity of the intracellular environment with regard to substrate availability and regulation. The quantity of lactate dehydrogenase was not

determined in each of the age groups so it is also possible that the aged cells express higher levels of the enzyme. In any case, age-dependent differences in glucose metabolism suggest a fundamental phenotypic divergence in tendon cell aging.

In consideration of the tendon as a contingent structure of the muscle-tendon unit, the significance of glucose metabolism and lactate production may have broader implications on tendon function. Exercise induced lactate production and subsequent pH decline in proportion to intensity has been known for many years [28]. Both the presence of lactate and a reduction in pH has been shown to modulate the force generation of the muscle-tendon unit and has demonstrated a protective function in response to muscle fatigue [29]. Lactate production may play an important role in the modulation of extracellular matrix as well. Lactic acid has been shown to enhance collagen production of flexor tendon cells [30]. Acidic environments can also activate key architectural proteases, such as matrix metalloproteinases, which degrade extracellular matrix [31]. Age-related changes in cellular metabolism may have complex structural and functional consequences in the development and acceleration of tendinopathy. For this reason, metabolic insights should be taken into consideration when trying to enhance tendon repair. Material choice, specifically polylactic acid (PLA), of tissue constructs may have an effect on modulating the native tendon cell population when the construct begins to degrade in vivo.

Oxidative metabolism was also investigated to compliment the previous assessment of anaerobic glycolysis. Mitochondrial membrane dyes were employed to semi-quantitatively evaluate mitochondrial function. Both JC-1 and CMXRos fluorescence, a carbocynanine-based dye and a rosamine-based dye respectively, are dependent on mitochondrial potential. JC-1 is

fluorescent at two distinct wavelengths depending on the formation of aggregates. Aggregates of the dye form when the monomer is taken up into the membrane of coupled and polarized mitochondria, both are healthy and functional characteristics of the organelle [32]. Depolarization is indicated by a decrease in the red to green fluorescence of JC-1.

Both dyes indicated slightly weaker mitochondrial membrane polarization in the 22-month tendon cells. Membrane electrochemical potential, or simply polarization, is the essential driving force for ATP production and plays significant roles in other bioenergetic functions of the mitochondria[23]. Loss of mitochondrial membrane potential has been demonstrated in age-related loss of function studies in cells from other rat tissues[33]. The data demonstrates a small loss of polarization with age, but must be carefully considered because the physiological significance is unclear. Direct measurement of the membrane potential would determine whether the differences are large enough to be physiologically relevant.

Cytochrome C Oxidase Subunit IV (COXIV) is an essential subunit of the fourth mitochondrial protein complex, which catalyzes the last reaction of electron transport to convert molecular oxygen to water [34]. Total protein was isolated from the cell cultures and western blot was performed to determine protein levels COXIV. COXIV was chosen as a representative mitochondrial protein essential to oxidative phosphorylation because it is necessary in the assembly of a functional complex IV[34]. Western blots were normalized by total protein and were reproducibly repeated four separate times because GAPDH and alpha-tubulin proved to be unreliable housekeeping genes under variable media conditions. The western blot analysis revealed consistent levels of mitochondrial protein between the age groups when maintained in glucose-supplemented media. In the pyruvate-supplemented

culture media, the aged tenocytes display a significant increase in COXIV protein. The increase in response to changes in media suggests the importance of glucose availability to the metabolic phenotype of the aged cells. Pyruvate-induced increases in COXIV expression has been shown in other cell types such as C2C12 myopblasts, where it was suggested that excessive pyruvate can actually be deleterious to metabolic function requiring an up-regulation mitochondrial machinery to compensate for metabolic debt [35]. Interestingly, the juvenile tendon cells show no COXIV expression variation in response to glucose availability.

ATP quantification demonstrated a slight variation in ATP between the 22-month and 1-month tendon cells. Again the physiological significance of a small decline of ATP in the aged tenocytes is debatable. The decline in ATP luminescence is only about 8% and is not definitively indicative of ATP deficiency in aged tendon cells.

Dichlorodihydrofluorescein diacetate (DCFDA) fluorescence indicated a significant decrease in reactive oxygen species in the 22-month tendon cells. This decrease in ROS could be attributed to reduced mitochondrial activity in aging tenocytes, which would also partially explain the decrease in ATP production because the ATP yield from oxidative phosphorylation far exceeds that of glycolysis. Mitochondria are one of the major sources of ROS in the majority of cell types excluding macrophages and other immune cells[23]. In order to address the plausibility of reduced mitochondrial activity to explain the depletion in ROS and ATP, we measured oxygen consumption, the results are explained below, but do not indicate any age-related deficiency in oxygen consumption under normal cell culture conditions.

Oxygen consumption of cultured cells provides a key functional assessment of mitochondrial oxidative phosphorylation [36]. Oxygen consumption rate (OCR) experiments

were carried out in the presence of a specific progression of mitochondrial inhibitors to provide a more detailed inspection of the oxygen consumption profile, which provides a fairly holistic examination of aerobic activity. Importantly, all of the experiments were carried out in identical assay media such that the cells from each group had identical conditions of substrate availability. Initial readings were taken to generate a baseline oxygen consumption of the experimental groups. The baseline oxygen consumption measurements are arguably the most valuable pieces of information from the mitochondrial stress test because they are representative of the native state of the cells, prior to pharmacological inhibition. The older cells exhibited higher levels of cellular respiration than the juvenile cells when cultured in glucose-supplemented media and this trend was conserved even in the presence of pharmacological inhibitors. Glucose-deprivation revealed a divergent response in OCR between the two age groups; the cells from the 22-month rats exhibited a decrease in OCR while the cells from the 1-month rats exhibited an increase in OCR.

After establishing baseline oxygen consumption rates, oligomycin was added to inhibit ATP-synthase, restrict proton flux, and inhibit the synthesis of mitochondrial ATP [37]. The corresponding decline in oxygen consumption is due to the arrest of ATP turnover. This decline was shown to be consistent in all of the groups presented in the data above.

Next the uncoupler FCCP was added. FCCP is an amphipathic molecule that accumulates in phospholipid bilayers and can increase the permeability of the membranes. In the mitochondrial membrane, this results in proton permeability and the uncoupling of the electron transport chain from production of ATP via ATP synthase. The maximal respiratory capacity results when the electron transport chain is intact and can transfer electrons for the reduction

of oxygen, but is not restricted by the rate of ATP production. The maximal respiratory capacity of the groups showed key differences. Again the divergent response to glucose-deprivation was apparent in the FCCP-induced determination of maximal oxygen consumption.

Lastly, rotenone and antimycin A were added as potent electron transport inhibitors at Complex I. Without electron transport, oxygen is not consumed and the resultant consumption value is attributed to non-mitochondrial oxygen consumption. The data indicates that non-mitochondrial respiration contributed minimally to the total oxygen consumption and remained relatively proportional despite the choice of media in all of the groups of interest.

The oxygen consumption results are consistent with the JC-1, CMXRos, COXIV and ATP quantification results. All of these experimental techniques to assess mitochondrial function do not conclusively indicate any major deficiencies of the aged tenocytes. However the glycolytic and mitochondrial examinations demonstrate key age-related differences in glucose-dependent metabolic behavior. The effects of depleting the growth medium of glucose are summarized in Table 1 for each age group.

TABLE 1. **Cell Response to Glucose Starvation**	22-month Tendon Cells	1-month Tendon Cells
Proliferation	↓	≈
LDH Activity	↓	≈
COXIV protein	↑	≈
Maximal Oxygen Consumption	↓	↑

It is clear that glucose plays a fundamental role in bioenergetic homeostasis. Furthermore, the reduction in proliferation, lactate dehydrogenase activity, and maximal

oxygen consumption in response to glucose starvation suggests that glucose is a key energy-providing substrate for the 22-month tendon cells, which agrees strongly with our previous findings that suggest a prominent role for glycolysis in normal metabolism. Furthermore, the age-dependent OCR, LDH, and COXIV responses to glucose-deprivation suggest tight interdependence of glycolysis and oxidative phosphorylation in the cells isolated from the older rats. In contrast, the juvenile cells exhibit metabolic flexibility through their consistent functional performance across media conditions. The juvenile cells are able to adapt to different media conditions, in terms of proliferation, LDH activity, and oxidative function, which suggests a loose coupling or independence of the two metabolic pathways.

In summary, the aged tendon cells are sensitive to changes in substrate and rely on glycolysis as an essential mediator of energy production. Juvenile tendon cells do not show the same sensitivity to glucose starvation. The culmination of the metabolic data displayed here implicates distinct bioenergetic phenotypes that change with aging. Older tendon cells are more glycolytic and more sensitive to changes in glucose availability whereas juvenile tendon cells are able to maintain a robust metabolic phenoytpe in multiple culture conditions.

Part 3: MMP Activity, Decorin, and the Regulation of Tendon Extracellular Matrix

Introduction

Maintenance and remodeling of extracellular matrix not only requires collagen synthesis, but also requires the degradation of structural proteins to accomplish extracellular matrix homeostasis. Matrix degradation by tenocytes is accomplished primarily through the production and regulation of matrix metalloproteinases [38]. Matrix metalloproteinases are a family of zinc dependent endopeptidases that are proteolytic at neutral pH [39]. Various members of the MMP family cleave a variety of substrates including fibrillar collagens, non-fibrillar collagens, degraded collagen, and proteoglycans among others [40].

MMP proteolytic activity enables two essential functions of tissue remodeling: cell migration and architectural restructuring [39]. MMPs are regulated at multiple stages. The most common form of early regulation is the translational inclusion of an auto-inhibitory pro-domain that must be destabilized or cleaved in order to activate the latent MMPs [39]. A second and later form of regulation is accomplished by the association of tissue inhibitors of matrix metalloproteinases or TIMPs. TIMPs inactivate MMPs by forming a 1:1 complex with the active zinc-containing catalytic site of the MMP [41]. MMP production and regulation is a cell-mediated means of tunable degradation and is essential to matrix remodeling in tendon. Altered MMP expression and activity has been implicated in the progression of tendinopathic tissue [40].

Age-related tendinopathy is characterized by distinct architectural changes that were discussed in part 1. One of the key pathological features of tendinopathy is the increase in collagen synthesis and simultaneous hyperactivity of MMPs [42]. These changes in matrix

production and degradation along with clinical observations of fibrotic disorganization suggest regulatory oversight in the progression of tendinopathy. In this last section, we aimed to elaborate on purely age-dependent changes in matrix degradation by studying MMP activity profiles of tendon cells isolated from 1-month and 22-month old rats in vitro. Moreover, we investigated the age-dependent shifts in the synthesis of structural proteins by examining mRNA expression in two groups of cells. These results were then discussed as they pertained to the degenerative features of the tissue identified in part 1.

Methods:

Generic MMP activity:

Six-well plates were plated with tendon cells at 10,000 cells/cm^2 and grown for 4 days in culture. Conditioned media from cultures isolated from both age groups was collected after the cells had reached confluence (after the fourth day). The media was spun down and the supernatant was used as the testing sample. All MMP containing samples were first activated with 1mM APMA and then incubated at 37°C for one hour. The Sensolyte 520 Generic MMP Assay Kit (AnaSpec) was used to determine the relative activities in the culture media from cells of the two age groups in accordance with the manufacturer's instructions. The kit is based on a 5-FAM fluorescent peptide that is quenched by a QXL520 construct when intact. A cleavage site is maintained with broad spectrum MMP specificity between the two peptide constructs. Upon cleavage by non-specific MMPs, the quencher is released and fluorescence is measured at 490 nm/520 nm. A standard is provided with the kit and a standard plot was constructed to determine the concentration of cleaved substrate. Fluorescence was recorded continuously for

approximately 35 minutes and the data was converted utilizing the standard plot. All groups were performed in quadruplicate and normalized by cell number.

Gelatin Zymography:

Gel electrophoresis was carried out using the Mini PROTEAN 3 system (Biorad) under denaturing conditions. Gels contained 7.5% polyacrylamide, 1 mg/mL gelatin, 375 mM Tris-HCl pH 8.8, 0.1% SDS. The gels were polymerized by adding 0.05% TEMED and 0.5% ammonium persulfate. The stacking gel contained 4% polyacrylamide with the same concentration of gelatin as the running gel. The running buffer consisted of 25 mM Tris, 192 mM glycine, and 3.47 mM SDS at pH 8.3. Media samples taken from confluent 6-well plate cultures grown for (4-5 days) were diluted 1:1 in 1M Tris pH 6.8 containing 50% glycerol and .04% bromphenol blue. After electrophoresis gels were submerged for 30 mins in 2.5% TritonX-100 to exchange the SDS and renature the MMPs. The gels were then incubated for up to 48 hours in 50 mM Tris-HCl, 50 mM NaCl, 10 mM $CaCl_2$, 0.02% Brij-L23 at pH 7.6 to activate the latent and active forms of the MMPs. Finally, gels were stained with 0.25% Coumassie blue G-250, destained with 20% methanol and 10% acetic acid, and analyzed using ImageJ to quantify the relative density of the bands.

Collagen & Decorin Gene Expression

Real-time PCR was performed to determine gene expression of collagen I, collagen III, and decorin. Total RNA was prepared from $5X10^5$ tendon cells from both 1-month and 22-month rats. The cells were lysed after reaching approximately 80% confluence (48-72 hours of growth on tissue culture plastic). RNeasy (Qiagen) isolation kit was used to isolate the RNA according to the manufacturer's instructions. Reverse transcription of total RNA was carried out in three consecutive steps: annealing (70°C for 10min), synthesis (42°C for 60min), and inactivation

(95°C for 5min). Real-time PCR was accomplished using iQ SYBR Green Supermix (Biorad). The 25uL reaction volume contained forward and reverse primers at a final concentration of 300 nM each. A six 10-fold dilution series was included on each 96-well PCR plate. The plates were sealed with optical adhesive plastic (Biorad) and spun down prior to real-time PCR analysis. Each sample was analyzed in triplicate. Forty cycles were carried out, after an initial 5 minute denaturing step, consisting of a denaturation step (95°C for 30s), an annealing step (primer specific for 30s), and a lengthening step (72°C for 30s). The forty cycles were followed by a melting curve which was inspected for quality assurance. The C_T values were set based on the linear logarithmic phase of the fluorescence curve. A standard curve was constructed based on linear regression of the dilution series and the relative expression levels were quantified. All expression values were normalized to 18s expression.

Table 2. RT-PCR Primer Sequences

Gene	Abbreviation	Primer Sequence	Annealing Temp
collagen 1	*Col1a1*	Fwd: AGGCTTTGATGGACGCAATG	58°C
		Rev: GCGGCTCCAGGAAGACC	
collagen 3	*Col3a1*	Fwd: CCATGGGTCCCAGAGGGGCT	57°C
		Rev: GGGACCTGGTTGCCCGTCAC	
decorin	*Dcn*	Fwd: TGGCAGTCTGGCTAATGT	58°C
		Rev: ACTCACGGCAGTGTAGGA	
18s	*18s*	Fwd: CGGCGACGACCCATTCGAAC	58°C
		Rev: GAATCGAACCCTGATTCCCCGTC	

Results:

The fluorometric and zymographic investigations (Fig. 17 and Fig. 18 respectively) of tenocyte cell culture media confirm that the broad range activity of matrix metalloproteinases is enhanced in the cells isolated from the 22-month rat tendon. The zymographic breakdown by molecular weight offers a more specific examination of MMP activity by demonstrating the enhanced activity of the gelatinase, MMP-9, and reduced activity of the pro-collagenase, Pro-

MMP1. The pro forms of MMPs are a latent precursor form requiring activation, but in zymography SDS denaturing also causes activation, which allows for the quantification of proMMPs. Gelatin zymography demonstrates the down regulation of the pro-form of MMP-1.

Gene expression analysis of the primary structural components of tendon including, decorin, collagen I, and collagen III revealed a large up-regulation of the decorin gene in the cells isolated from the 22-month rats (Fig. 19). Upregulated expression was also demonstrated for the collagen III gene.

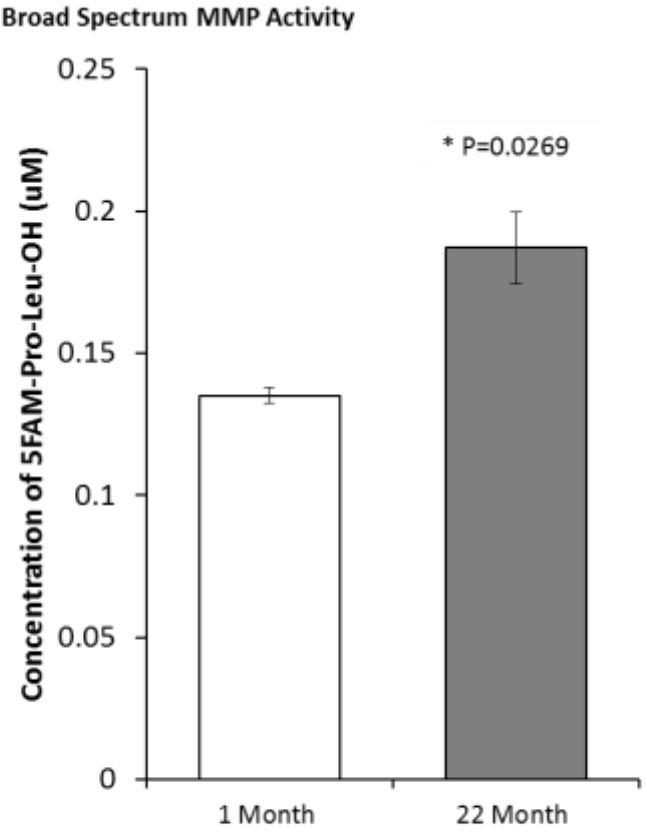

Figure 17. Matrix metalloproteinase (MMP) activity. Tendon cells isolated form 22 month rats displayed higher overall MMP activity. The data was based on assays of cell culture media. All data were normalized by cell number. The cells were allowed to reach confluence in 6-well plates (4-5days) before sampling the media.

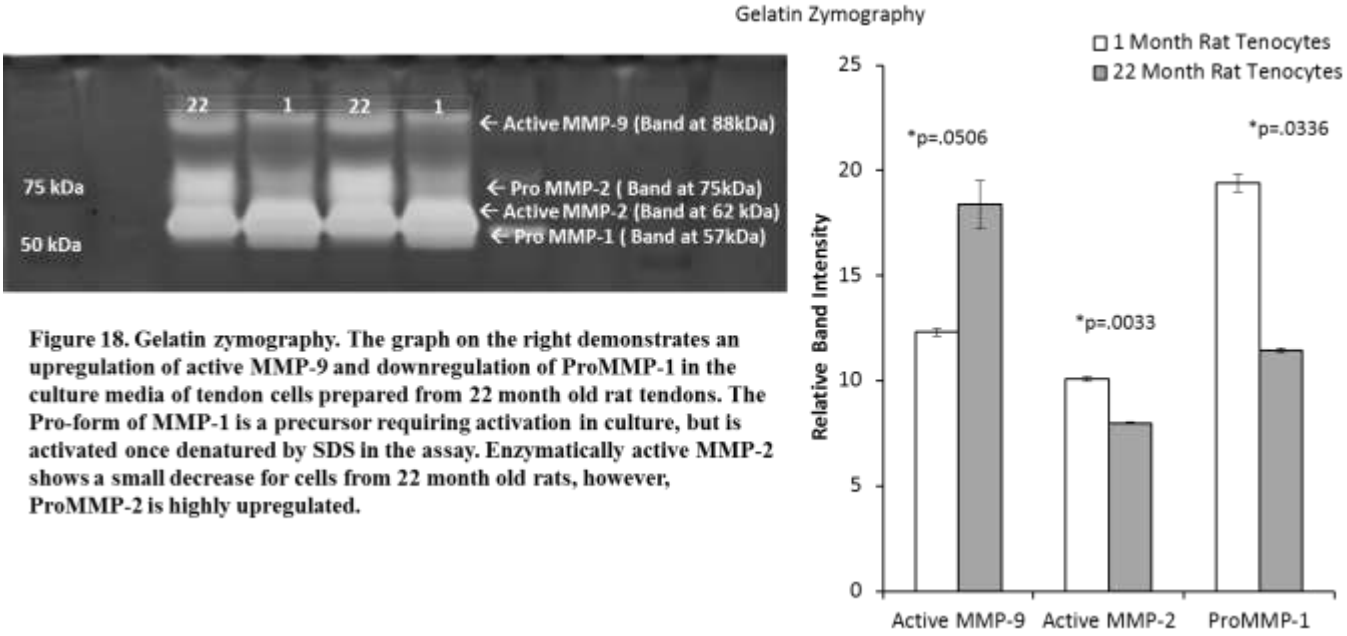

Figure 18. Gelatin zymography. The graph on the right demonstrates an upregulation of active MMP-9 and downregulation of ProMMP-1 in the culture media of tendon cells prepared from 22 month old rat tendons. The Pro-form of MMP-1 is a precursor requiring activation in culture, but is activated once denatured by SDS in the assay. Enzymatically active MMP-2 shows a small decrease for cells from 22 month old rats, however, ProMMP-2 is highly upregulated.

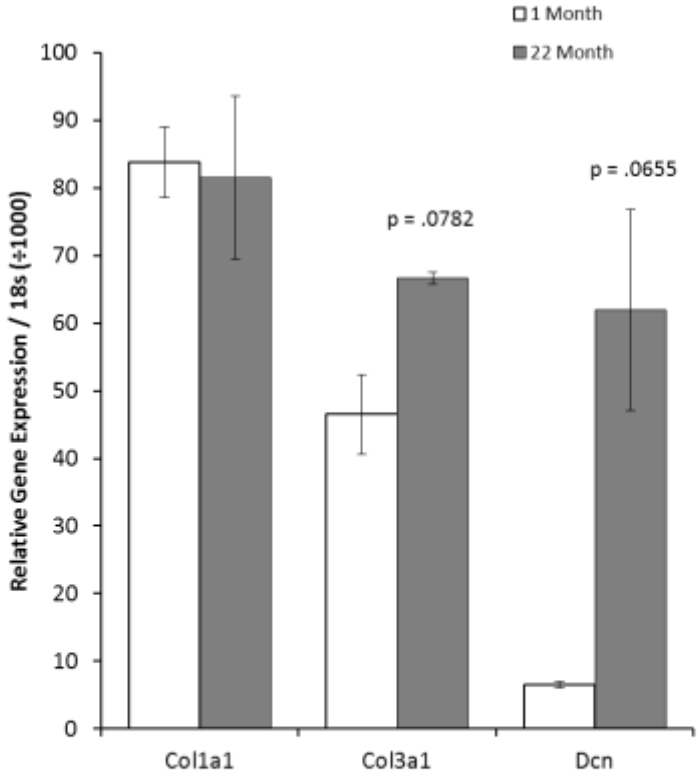

Figure 19. Expression of collagen and decorin genes. The graph above shows relative expression data normalized by18s RNA. The expression of 18s was much higher than any of the genes displayed so the data was normalized by 1000 to make the data more viewable. While expression of Col1a1 is not significantly different between the cells from old and young rats, there is an increase in the expression of Col3a1 and a dramatic increase in the expression of the decorin gene in the cells from 22-month old rats compared to cells isolated from 1-month rats.

Discussion:

Aged tendon displays a marked increase in MMP activity. The data from our study on aging agrees with many studies that demonstrate elevated MMP expression or activity in tendinopathic tissue [42], [43]. The up-regulation of MMP-9 and down-regulation of ProMMP-1 demonstrates a relative enhancement of gelatinolytic activity to collagenase activity. The down-regulation of pro-MMP1 indicates that there is a reduction in the production of the latent precursor form of MMP-1.

Gelatinolytic activity is responsible for the degradation of fibrillar, but denatured collagens; this is implicated as a response to the accumulation of degenerative tissue, but may also be involved as a mediator of age-related tendinopathy due to characteristic over activity. The rationale is clear for age-related dysregulation of the regulatory enzymes involved in extracellular matrix degradation and as a result the evidence may have broader consequences on the tissue architecture, and subsequent tissue function.

Interestingly, decorin is the most abundant proteoglycan in tendon and is a substrate of MMP-2, MMP-3, and MMP-7[44]. Decorin is a small leucine-rich proteoglycan that functions in the regulation of type-1 collagen fibril formation and is specifically thought to play a major role in the modulation of tendon fibril diameter[45]. Our findings are not surprising in that the increase in proMMP-2 in 22-month tenocytes is consistent with our TEM imaging that demonstrates abnormal fibril diameter in the aged tissue. Additionally, gene expression analysis shows a significant up-regulation of decorin expression suggesting a tenocyte-mediated response to reverse or mitigate the effect of decorin cleavage by elevated MMP-2. The absence of decorin, in decorin-knockout mice, results in the aggregation of large diameter fibrils and

multiple levels of fibril disorganization [46], which suggests decorin can prevent fibril dysregulation. However, there is no evidence for the efficacy of decorin to reverse fibril disorganization after it has developed; this may be one of several reasons that decorin gene over expression has been identified in the cells, but the fibrils remain disorganized in the tissue.

Exercise and injury also have acute effects on MMP production and activity and play a central role in regulating the remodeling process [43], [47].For example, acidification in local muscle-tendon microenvironments in response to exercise and oxygen depletion may have an immediate effect on MMP function by activating latent MMPs. The complexity of age-related degeneration in the context of extracellular matrix metabolism and specifically MMP function is augmented by long-term exercise and injury that accrues throughout the lifespan of the individual. A holistic examination of MMP metabolism should consider the contributions from multiple perspectives. Exercise, activity level, injury, muscle fiber-type, and other individual-specific characteristics should be considered in the evaluation of age-related degeneration.

Summary of Findings and Conclusions:

1. **Gross Cell Morphology and Characterization of Primary Rat Achilles Tendon Cells**
    a. Achilles tendon excised from 22-month rats displays many degenerative characteristics consistent with human Achilles tendinopathy including abnormal fibril diameter variability, tissue hypocellularity, and the incidence of chondroid metaplasia in the tendon midsubstance.
    b. Tendon-derived cell cultures from older rats are able to proliferate at rates equal to or higher than the cells isolated from tendon of younger rats in vitro. There was no significant difference in telomere length between the cells derived from each age group. The proliferative ability and comparable telomere length is not indicative of cellular senescence. The lack of proliferation in tissue from older rats indicated by histological evidence of hypocellularity and the replicative ability of the same cells isolated and grown in culture is paradoxical. If changes in extracellular matrix with age are responsible, at least in part, for the observed metabolic differences between cells derived from the tendons of young versus old rats then removal of the matrix may be the primary reason behind the observation that cells isolated from old tendons resume their proliferative capacity when placed in culture.
2. **Metabolic Investigation of Glycolytic Activation and Mitochondrial Function**
    a. Tendon cells from older rats are more glycolytically active than tendon cells isolated from younger rats. Specifically, the cellular extracts from the cultures contain higher levels of lactate and lactate dehydrogenase activity. The cells from older rats also grow faster in glucose-supplemented media than cells in glucose-deficient media.

b. Cells from the older animals are more sensitive to the presence of glucose in the growth media. Glucose-deficient media causes the tendon cells from older animals to reduce the levels of oxygen consumption, lactate dehydrogenase activity, and expression of COXIV protein.

c. The tendon cells from the younger animals demonstrate an adaptive and robust metabolic phenotype characterized by consistent proliferation, lactate dehydrogenase activity, and COXIV protein expression, regardless of the presence of glucose in the growth media.

d. Cells isolated from 1-month and 22-month rat tendons exhibit similar mitochondrial membrane polarization and express similar levels of COXIV protein in glucose-supplemented media. Neither age group shows a deficiency in oxygen consumption relative to the other group. The COXIV, oxygen consumption, and membrane polarization data do not indicate mitochondrial dysfunction in cells cultured in vitro from 22-month rat tendons.

3. MMP activity, decorin, and the regulation of tendon extracellular matrix

a. Tendon cell cultures display age-dependent patterns of matrix metalloproteinase activity. Cell culture media extracts from older rat tendon cells have a higher broad spectrum matrix metalloproteinase activity. Gel zymography demonstrated that these media extracts have elevated MMP-9 and proMMP-2 activities.

b. The expression of the decorin gene is elevated in cultures of cells prepared from the older animals. Decorin is a regulator of lateral fibril growth and the elevated decorin

data is consistent with the demand for cell-mediated regulation demonstrated in part 1 by collagen fibril diameter variability.

Further Studies:

This investigation provides a broad characterization of the metabolism of Achilles tendon cells isolated from aged rats. Two very interesting metabolic findings were identified within the context of age-related tendinopathy. First, the metabolic divergence of cells from the older tissue was established in terms of glycolytic and oxidative function. Extracellular metabolism was also investigated and age-related dysfunction was implicated in the deregulation of extracellular matrix synthesis and degradation. These two findings have opened the door for further investigation of tendon cell metabolism in an aged rat model.

The most interesting result, in my opinion, is the lack of metabolic flexibility and more specifically the strong dependence of the cellular metabolism, in the older cells, on glucose availability. However, the complexity of energy metabolism, involving several simultaneous mechanisms with many interdependent metabolites, is extremely difficult to study in vitro, let alone in vivo, which makes this area of research particularly challenging. In fact, one of the fundamental weaknesses of this investigation, limiting the clinical relevance of the study, is the disconnect between the complexity of the tissue environment and the limitations of culture system in vitro. Further studies should be pursued in vivo to enhance the clinical relevance with respect to elucidating mechanisms of age-related pathology and advancing the development of non-invasive therapeutics for tendinopathy.

A follow-up investigation to explore the role of decorin in collagen fibril regulation and the development of age-related tendinopathy is a more pursuable area of research, in my

opinion. This investigation should probe both the spatial and temporal expression patterns of decorin. Additionally, both the gene and protein expression should be determined in order to identify lapses in decorin regulation that may lead to insights in mechanistic relationships. By studying the temporal expression over multiple age groups (juvenile, middle-aged, aged) and identifying the spatial profile of decorin expression in the tissue via immunochemical localization, the development of tissue dysregulation can be mapped in parallel with the aging of the tissue. Furthermore, by studying spatial relationships in vivo, the complexity of the extracellular matrix can be preserved, while examining the role of cell-mediated dysfunction in disease progression.

Clinical Translation:

The in vitro investigation provides a useful perspective on the condition of the native tendon cell population. These cells are viable therapeutic targets to enhance tendon repair and alleviate tendinopathies that afflict older individuals. The evidence detailed in this study support the notion that tenocytes in older animals are not senescent. This evidence of replicative potential especially conveys promise for cell-targeted therapies. The ability of the cells to proliferate at levels equal to that of the juvenile group suggests that the hypocellularity of tenocytes observed in degenerative tissue is not restricted by fundamental proliferative potential. One implicated inhibitor of migration and proliferation in vivo may be attributed to matrix architecture such as density, cross linking, fibril size, and possibly other parameters.

The establishment of metabolic phenotypes and specifically the glucose-sensitivity of aged tendon cells demonstrate the importance of nutrient availability in the adult tendon. Blood supply in Achilles tendon is limited and originates at both ends of the tendon, at the

insertion and at the muscular junction as well as throughout the paratenon [48]. The mid-substance of the tendon is poorly vascularized and the capillaries, which are crucial to nutrient exchange, cannot penetrate the collagen matrix [2]. Degenerative tissues often have increased fibrosis, large fibril diameters, and reduced organization, which could have a significant impact on nutrient dispersion throughout the tissue. The glucose-sensitive phenotype of tendon cells from older animals implicates that treatments aimed at enhancing nutrient delivery may be efficacious in modulating cellular responses.

The characterization of the rat Achilles tendon and the effect of aging, which is consistent with the progression of tendinopathy in humans, lay the foundation for developing a model system of age-related degeneration that can be used to assess experimental therapeutics in vivo. The in vivo system can be assessed by determining tissue cellularity, collagen fibril alignment, and collagen fibril diameter. The MMP activity of excised tissue segments could also be assessed to determine if the treatment has reduced the gelatinolytic hyperactivity that is associated with degenerative tissue.

The conclusions from this research can be used to investigate the design and implementation of new therapeutic strategies for Achilles tendon repair and degeneration. Metabolic insights such as glucose sensitivity and lactate production can be incorporated into the design of novel, bioactive surgical constructs that account for age-related metabolic dysfunction of tendinopathy. The effect of exercise on the metabolism of tendon cells and the effect on tendon tissue as a whole can be studied to delineate therapy from overuse. The results of this investigation contribute to a growing field of work on age-related musculoskeletal pathologies that will help clinicians and researchers alike to understand

fundamental metabolic dynamics as they pertain to an expanding population of aging individuals.

References:

[1] M. Paavola, P. Kannus, T. A. H. Järvinen, K. Khan, L. Józsa, and M. Järvinen, "Achilles Tendinopathy," *J Bone Joint Surg Am*, vol. 84, no. 11, pp. 2062–2076, Nov. 2002.

[2] M. O'Brien, "Anatomy of Tendons," in *Tendon Injuries*, N. M. M. FRCS(Orth) MS, P. R. MD, and W. B. L. MD, Eds. Springer London, 2005, pp. 3–13.

[3] L. E. Dahners, "Growth and Development of Tendons," in *Tendon Injuries*, N. M. M. FRCS(Orth) MS, P. R. MD, and W. B. L. MD, Eds. Springer London, 2005, pp. 22–24.

[4] G. Zhang, B. B. Young, Y. Ezura, M. Favata, L. J. Soslowsky, S. Chakravarti, and D. E. Birk, "Development of tendon structure and function: regulation of collagen fibrillogenesis," *J Musculoskelet Neuronal Interact*, vol. 5, no. 1, pp. 5–21, Mar. 2005.

[5] J. H. Yoon and J. Halper, "Tendon proteoglycans: biochemistry and function," *J Musculoskelet Neuronal Interact*, vol. 5, no. 1, pp. 22–34, Mar. 2005.

[6] P. J. Neame*, C. J. Kay, ** D. J. McQuillan, M. P. Beales, and J. R. Hassell, "Independent modulation of collagen fibrillogenesis by decorin and lumican," *CMLS, Cell. Mol. Life Sci.*, vol. 57, no. 5, pp. 859–863, May 2000.

[7] A. Hildebrand, M. Romaris, L. M. Rasmussen, D. Heinegard, D. R. Twardzik, W. A. Border, and E. Ruoslahti, "Interaction of the small interstitial proteoglycans biglycan, decorin and fibromodulin with transforming growth factor beta.," *Biochem J*, vol. 302, no. Pt 2, pp. 527–534, Sep. 1994.

[8] M. Benjamin, E. Kaiser, and S. Milz, "Structure-function relationships in tendons: a review," *Journal of Anatomy*, vol. 212, no. 3, pp. 211–228, 2008.

[9] P. Kannus, "Structure of the tendon connective tissue," *Scand J Med Sci Sports*, vol. 10, no. 6, pp. 312–320, Dec. 2000.

[10] P. Sharma and N. Maffulli, "Biology of tendon injury: healing, modeling and remodeling," *J Musculoskelet Neuronal Interact*, vol. 6, no. 2, pp. 181–190, Jun. 2006.

[11] N. Maffulli, P. Sharma, and K. L. Luscombe, "Achilles tendinopathy: aetiology and management," *J R Soc Med*, vol. 97, no. 10, pp. 472–476, Oct. 2004.

[12] P. Kannus, M. Paavola, and L. Józsa, "Aging and degeneration of tendons," *Tendon injuries: basic science and clinical medicine, London*, pp. 25–31, 2005.

[13] W. Tsai, H. Chang, T. Yu, C. Chien, L. Fu, F. Liang, and J. S. Pang, "Decreased proliferation of ageing tenocytes is associated with down-regulation of cellular senescence-inhibited gene and up-regulation of p27," *Journal of Orthopaedic Research*.

[14] R. Strocchi, V. De Pasquale, S. Guizzardi, P. Govoni, A. Facchini, M. Raspanti, M. Girolami, and S. Giannini, "Human Achilles tendon: morphological and morphometric variations as a function of age," *Foot Ankle*, vol. 12, no. 2, pp. 100–104, Oct. 1991.

[15] A. J. Bailey, R. G. Paul, and L. Knott, "Mechanisms of maturation and ageing of collagen," *Mechanisms of Ageing and Development*, vol. 106, no. 1–2, pp. 1–56, Dec. 1998.

[16] M. de Mos, B. van El, J. DeGroot, H. Jahr, H. T. M. van Schie, E. R. van Arkel, H. Tol, R. Heijboer, G. J. V. M. van Osch, and J. A. N. Verhaar, "Achilles Tendinosis Changes in Biochemical Composition and Collagen Turnover Rate," *Am J Sports Med*, vol. 35, no. 9, pp. 1549–1556, Sep. 2007.

[17] M. de Mos, W. Koevoet, H. T. M. van Schie, N. Kops, H. Jahr, J. A. N. Verhaar, and G. J. V. M. van Osch, "In Vitro Model to Study Chondrogenic Differentiation in Tendinopathy," *Am J Sports Med*, vol. 37, no. 6, pp. 1214–1222, Jun. 2009.

[18] M. Benjamin and J. R. Ralphs, "Fibrocartilage in tendons and ligaments - an adaptation to compressive load," *Journal of Anatomy*, vol. 193, no. 4, pp. 481–494, Nov. 1998.

[19] S. M. Arnesen and M. A. Lawson, "Age-related changes in focal adhesions lead to altered cell behavior in tendon fibroblasts," *Mechanisms of Ageing and Development*, vol. 127, no. 9, pp. 726–732, Sep. 2006.

[20] N. Maffulli, J. Wong, and L. C. Almekinders, “Types and epidemiology of tendinopathy,” *Clin Sports Med*, vol. 22, no. 4, pp. 675–692, Oct. 2003.
[21] E. Ippolito, P. G. Natali, F. Postacchini, L. Accinni, and C. De Martino, “Morphological, Immunochemical, and Biochemical Study of Rabbit Achilles Tendon at Various Ages,” *J Bone Joint Surg Am*, vol. 62, no. 4, pp. 583–598, Jun. 1980.
[22] M. Abate, C. Schiavone, V. Salini, and I. Andia, “Occurrence of tendon pathologies in metabolic disorders,” *Rheumatology*, Jan. 2013.
[23] M. R. Duchen, “Mitochondria in health and disease: perspectives on a new mitochondrial biology,” *Molecular Aspects of Medicine*, vol. 25, no. 4, pp. 365–451, Aug. 2004.
[24] M. Tsuzaki, D. Bynum, L. Almekinders, X. Yang, J. Faber, and A. j. Banes, “ATP modulates load-inducible IL-1β, COX 2, and MMP-3 gene expression in human tendon cells,” *Journal of Cellular Biochemistry*, vol. 89, no. 3, pp. 556–562, 2003.
[25] U. G. Longo, F. Olivia, V. Denaro, and N. Maffulli, “Oxygen species and overuse tendinopathy in athletes,” *Disability & Rehabilitation*, vol. 30, no. 20–22, pp. 1563–1571, Jan. 2008.
[26] G. A. C. Murrell, “Oxygen free radicals and tendon healing,” *J Shoulder Elbow Surg*, vol. 16, no. 5 Suppl, pp. S208–214, Oct. 2007.
[27] C. L. Markert, “Lactate dehydrogenase. Biochemistry and function of lactate dehydrogenase,” *Cell Biochem. Funct.*, vol. 2, no. 3, pp. 131–134, Jul. 1984.
[28] K. Sahlin, R. C. Harris, B. Nylind, and E. Hultman, “Lactate content and pH in muscle samples obtained after dynamic exercise,” *Pflugers Arch.*, vol. 367, no. 2, pp. 143–149, Jan. 1976.
[29] O. B. Nielsen, F. de Paoli, and K. Overgaard, “Protective effects of lactic acid on force production in rat skeletal muscle,” *The Journal of Physiology*, vol. 536, no. 1, pp. 161–166, 2001.
[30] M. B. Klein, H. Pham, N. Yalamanchi, and J. Chang, “Flexor tendon wound healing in vitro: The effect of lactate on tendon cell proliferation and collagen production,” *The Journal of Hand Surgery*, vol. 26, no. 5, pp. 847–854, Sep. 2001.
[31] R. Visse and H. Nagase, “Matrix Metalloproteinases and Tissue Inhibitors of Metalloproteinases Structure, Function, and Biochemistry,” *Circulation Research*, vol. 92, no. 8, pp. 827–839, May 2003.
[32] M. Reers, T. W. Smith, and L. B. Chen, “J-aggregate formation of a carbocyanine as a quantitative fluorescent indicator of membrane potential,” *Biochemistry*, vol. 30, no. 18, pp. 4480–4486, May 1991.
[33] T. M. Hagen, D. L. Yowe, J. C. Bartholomew, C. M. Wehr, K. L. Do, J.-Y. Park, and B. N. Ames, “Mitochondrial decay in hepatocytes from old rats: Membrane potential declines, heterogeneity and oxidants increase,” *PNAS*, vol. 94, no. 7, pp. 3064–3069, Apr. 1997.
[34] Y. Li, J.-S. Park, J.-H. Deng, and Y. Bai, “Cytochrome c Oxidase Subunit IV is Essential for Assembly and Respiratory Function of the Enzyme Complex,” *J Bioenerg Biomembr*, vol. 38, no. 5–6, pp. 283–291, Dec. 2006.
[35] A. Philp, J. Perez-Schindler, C. Green, D. L. Hamilton, and K. Baar, “Pyruvate suppresses PGC1α expression and substrate utilization despite increased respiratory chain content in C2C12 myotubes,” *Am J Physiol Cell Physiol*, vol. 299, no. 2, pp. C240–C250, Aug. 2010.
[36] M. D. Brand and D. G. Nicholls, “Assessing mitochondrial dysfunction in cells,” *Biochem J*, vol. 435, no. Pt 2, pp. 297–312, Apr. 2011.
[37] D. G. Nicholls, V. M. Darley-Usmar, M. Wu, P. B. Jensen, G. W. Rogers, and D. A. Ferrick, “Bioenergetic Profile Experiment using C2C12 Myoblast Cells,” *Journal of Visualized Experiments*, no. 46, Dec. 2010.
[38] G. Riley, “Tendinopathy—from basic science to treatment,” *Nature Clinical Practice Rheumatology*, vol. 4, no. 2, pp. 82–89, 2008.
[39] A. Page-McCaw, A. J. Ewald, and Z. Werb, “Matrix metalloproteinases and the regulation of tissue remodelling,” *Nature Reviews Molecular Cell Biology*, vol. 8, no. 3, pp. 221–233, Mar. 2007.

[40] M. Magra and N. Maffulli, “Matrix metalloproteases: a role in overuse tendinopathies,” *Br J Sports Med*, vol. 39, no. 11, pp. 789–791, Nov. 2005.
[41] C. E. Brinckerhoff and L. M. Matrisian, “Matrix metalloproteinases: a tail of a frog that became a prince,” *Nat Rev Mol Cell Biol*, vol. 3, no. 3, pp. 207–214, Mar. 2002.
[42] A. Scott, K. M. Khan, J. L. Cook, and V. Duronio, “Human Tendon Overuse Pathology: Histopathologic and Biochemical Findings,” in *Tendinopathy in Athletes*, S. L.-Y. W. DSc, P. A. F. H. R. MD, and S. P. A. DVM, Eds. Blackwell Publishing Ltd, 2008, pp. 69–84.
[43] E. Karousou, M. Ronga, D. Vigetti, A. Passi, and N. Maffulli, “Collagens, Proteoglycans, MMP-2, MMP-9 and TIMPs in Human Achilles Tendon Rupture,” *Clin Orthop Relat Res*, vol. 466, no. 7, pp. 1577–1582, Jul. 2008.
[44] K. Imai, A. Hiramatsu, D. Fukushima, M. D. Pierschbacher, and Y. Okada, “Degradation of decorin by matrix metalloproteinases: identification of the cleavage sites, kinetic analyses and transforming growth factor-beta1 release,” *Biochem. J.*, vol. 322 (Pt 3), pp. 809–814, Mar. 1997.
[45] G. Zhang, Y. Ezura, I. Chervoneva, P. S. Robinson, D. P. Beason, E. T. Carine, L. J. Soslowsky, R. V. Iozzo, and D. E. Birk, “Decorin regulates assembly of collagen fibrils and acquisition of biomechanical properties during tendon development,” *Journal of Cellular Biochemistry*, vol. 98, no. 6, pp. 1436–1449, 2006.
[46] K. G. Danielson, H. Baribault, D. F. Holmes, H. Graham, K. E. Kadler, and R. V. Iozzo, “Targeted Disruption of Decorin Leads to Abnormal Collagen Fibril Morphology and Skin Fragility,” *J Cell Biol*, vol. 136, no. 3, pp. 729–743, Feb. 1997.
[47] M. Kjaer, H. Langberg, B. F. Miller, R. Boushel, R. Crameri, S. Koskinen, K. Heinemeier, J. L. Olesen, S. Døssing, M. Hansen, S. G. Pedersen, M. J. Rennie, and P. Magnusson, “Metabolic activity and collagen turnover in human tendon in response to physical activity,” *J Musculoskelet Neuronal Interact*, vol. 5, no. 1, pp. 41–52, Mar. 2005.
[48] I. M. Ahmed, M. Lagopoulos, P. McConnell, R. W. Soames, and G. K. Sefton, “Blood supply of the achilles tendon,” *Journal of Orthopaedic Research*, vol. 16, no. 5, pp. 591–596, 1998.